Quaternary Science Reviews 300 (2023) 107874

Contents lists available at ScienceDirect

Quaternary Science Reviews

journal homepage: www.elsevier.com/locate/quascirev

Hydroclimate variability in the Madagascar and Southeast African summer monsoons at the Mid- to Late-Holocene transition

Nick Scroxton [a, b, *], Stephen J. Burns [a], David McGee [b], Laurie R. Godfrey [c], Lovasoa Ranivoharimanana [d], Peterson Faina [d], Benjamin H. Tiger [b, e]

[a] Department of Geosciences, 611 North Pleasant Street, University of Massachusetts Amherst, MA 01030, USA
[b] Department of Earth, Atmospheric and Planetary Sciences, Massachusetts Institute of Technology, 77 Massachusetts Avenue, Cambridge, MA 02139, USA
[c] Department of Anthropology, 240 Hicks Way, University of Massachusetts, Amherst, MA 01003, USA
[d] Mention Bassins Sédimentaires, Evolution, Conservation (BEC) – BP 906 – Faculté des Sciences, Université D'Antananarivo – 101 Antananarivo, Madagascar
[e] Woods Hole Oceanographic Institution, 266 Woods Hole Road, Woods Hole, MA 02543, USA

ARTICLE INFO

Article history:
Received 12 July 2022
Received in revised form
4 October 2022
Accepted 12 November 2022
Available online 1 December 2022

Handling Editor: Dr Mira Matthews

Keywords:
Holocene
Monsoon
Paleoclimatology
Africa
Madagascar
Speleothems
Stable isotopes
U–Th series
4.2 ka event
Data synthesis

ABSTRACT

The 4.2 ka event at the Mid- to Late-Holocene transition is often regarded as one of the largest and best documented abrupt climate disturbances of the Holocene. The event is most clearly manifested in the Mediterranean and Middle East as a regional dry anomaly beginning abruptly at 4.26 kyr BP and extending until 3.97 kyr BP. Yet the impacts of this regional drought are often extended to other regions and sometimes globally. In particular, the nature and spatial extent of the 4.2 ka event in the tropics have not been established. Here, we present a new stalagmite stable isotope record from Anjohikely, northwest Madagascar. Growing between 5.22 and 2.00 kyr BP, stalagmite AK1 shows a hiatus between 4.31 and 3.93 kyr BP (±40 and ± 35 yrs), replicating a hiatus in another stalagmite from nearby Anjohibe, and therefore indicating a significant drying at the Mid- to Late-Holocene transition. This result is the opposite to wet conditions at the 8.2 ka event, suggesting fundamentally different forcing mechanisms. Dry conditions are also recorded in sediment cores in Lake Malawi, Lake Masoko and the Tatos Basin on Mauritius, also in the southeast African monsoon domain. However, no notable event is recorded at the northern (equatorial East Africa) and eastern (Rodrigues) peripheries of the monsoon domain, while a wet event is recorded in sediment cores at Lake Muzi and Mkhuze Delta to the south. The spatial pattern is largely consistent with the modern rainfall anomaly pattern associated a with weak Mozambique Channel Trough and a northerly austral summer Intertropical Convergence Zone position. Within age error, the observed peak climate anomalies overlap with the 4.2 ka event. However regional hydrological change consistently begins earlier than a 4.26 kyr BP event onset. Gradual hydrological change frequently begins around 4.5 kyr BP, raising doubt as to whether any coherent regional hydrological change is merely coincident with the 4.2 ka event or part of a global climatic anomaly.

1. Introduction

Understanding and adapting to changes in water availability due to climate change is one of the most important challenges we face in the twenty-first century (Konapala et al., 2020; Loucks, 2022; Hanasaki et al., 2013). To do so, we must understand how rainfall responds to perturbation under boundary conditions close to modern (Cook et al., 2018; Narisma et al., 2007), and its impacts on societies. With significant Holocene climate variability now widely recognised (Fleitmann et al., 2003; Gupta et al., 2003; Mayewski et al., 2004; Wanner et al., 2011), the spatial patterns and processes of perturbations to rainfall in the recent past and at the decadal timescales relevant to modern climate change requires study (Nash et al., 2016). One of the largest climate perturbations of the Holocene is the so-called "4.2 ka event".

* Corresponding author. Present address: Irish Climate Analysis and Research Units, Department of Geography, Maynooth University, Maynooth, Co. Kildare, Ireland.,
E-mail addresses: nick.scroxton@mu.ie (N. Scroxton), sburns@geo.umass.edu (S.J. Burns), davidmcg@mit.edu (D. McGee), lgodfrey@umass.edu (L.R. Godfrey), ranivolova@gmail.com (L. Ranivoharimanana), petersonfaina@gmail.com (P. Faina), tigerb@mit.edu (B.H. Tiger).

https://doi.org/10.1016/j.quascirev.2022.107874
0277-3791/

The 4.2 ka event is best characterised and understood in the Mediterranean (Bini et al., 2019; Zanchetta et al., 2016) and Middle East (Kaniewski et al., 2018) where it is manifested as a widespread drought with abrupt onset and termination occurring between 4.26 and 3.97 kyr BP (Carolin et al., 2019) and linked to societal change in the Akkadian civilization (Höflmayer, 2017; Weiss et al., 1993; Weiss, 1997). However, both the spatial extent beyond the data-rich heartland of the northern hemisphere mid-latitudes, and the climate processes behind the 4.2 ka event are uncertain. The 4.2 ka event has been interpreted as one of the smallest forced climate anomalies of the Holocene, perhaps through a freshwater input into the north Atlantic (Wang et al., 2013) despite little evidence for a such an event (Bradley and Bakke, 2019). Alternatively, it has also been viewed as one of the largest unforced climate anomalies (i.e., natural variability) of the Holocene (Yan and Liu, 2019), driven by changes in the North Atlantic Oscillation. As a result of these uncertainties, the 4.2 ka event as a globally impacting megadrought and subsequent formal designation as the Middle to Late Holocene (Northgrippian to Meghalayan) boundary (Walker et al., 2018) has proved controversial (Helama and Oinonen, 2019; Middleton, 2018; Voosen, 2018; Ön et al., 2021).

There is therefore a compelling need to understand drought, and rainfall variability in general, at the Mid- to Late-Holocene transition, along with any potential association with the 4.2 ka event and societal change. This is particularly true in the tropics and southern hemisphere where there have been only a few detailed studies (Marchant and Hooghiemstra, 2004; Railsback et al., 2018, 2022). In the tropics, there may be conflation of the 4.2 ka event and what is now a widely recognised shift in tropical climate at 4.0 kyr BP (Denniston et al., 2013; Gagan et al., 2004; Giosan et al., 2018; Li et al., 2018; MacDonald, 2011; Marchant and Hooghiemstra, 2004; Toth and Aronson, 2019). We note that the conflation does not necessarily arise in the original articles: for example, Marchant and Hooghiemstra (2004) do not discuss the 4.2 ka event, the association was added later (e.g. Staubwasser and Weiss, 2006). The 4.0 kyr BP tropical climate shift is likely related to changes in sea surface temperature (SST) (Marchant and Hooghiemstra, 2004), tropical rainbelt width (Li et al., 2018), and/or the mean state of the El Niño Southern Oscillation (de Boer et al., 2014; Denniston et al., 2013; Gagan et al., 2004; MacDonald, 2011; Toth et al., 2012). The event was recently dated to 3.97 kyr BP (±80 yrs, 1 standard error) through regional principal component analysis in the Indian ocean basin (Scroxton et al., 2022). Well-dated, high-resolution, paleoclimate records should be able to distinguish the 4.2 ka event and a tropical climate shift at 4.0 kyr BP. Even in records with low dating precision, the shape of the anomaly may help distinguish these two climatic events. The 4.0 kyr BP tropical climate shift is a longer duration, often unidirectional, transition.

Also relevant to the 4.2 ka event is the response of tropical monsoons to the 8.2 ka event, an abrupt North-Atlantic cold event under interglacial boundary conditions often viewed as a greater magnitude version of the 4.2 ka event (Bond et al., 2001; Wang et al., 2013). In the Malagasy Summer Monsoon (MSM), part of the Southeast African Monsoon (SEAfM) domain, negative $\delta^{18}O$ anomalies are recorded in stalagmites from northwest Madagascar and interpreted as indicating wet conditions (Voarintsoa et al., 2019). This result fits with the idea of a southerly shift in mean ITCZ/tropical rainbelt position resulting from a cooler Northern Hemisphere and/or reduced Atlantic thermohaline circulation (Broccoli et al., 2006; McGee et al., 2014; Zhang and Delworth, 2005). Therefore, if the 4.2 ka event is forced from a North-Atlantic cold event via freshwater input (Wang et al., 2013) wet anomalies in the MSM and SEAfM more broadly are predicted. The expectation would be for negative stalagmite $\delta^{18}O$ anomalies in the MSM at the 4.2 ka event.

In this study we investigate whether the 4.2 ka event or 4 ka tropical climate shift can be seen in paleoclimate records in the SEAfM and MSM domains, and the direction of any change. We present a new stalagmite $\delta^{18}O$ record of monsoon variability from northwest Madagascar, alongside other climate records from the region. Stalagmites, secondary calcium carbonate cave deposits, are particularly suited for detecting Holocene climate variability due to their continuous growth, sub-decadal resolution, U–Th derived absolute age errors frequently less than 1%, and paleoclimate proxies for hydroclimate variability such as stable oxygen isotopes ($\delta^{18}O$) (Fairchild and Baker, 2012; Lachniet, 2009; McDermott, 2004).

2. Regional setting

Seasonal cycle: Adjacent to the southwest Indian Ocean, the SEAfM and MSM are driven by the annual southwards migration of the Intertropical Convergence Zone (ITCZ) during austral summer (Nov–Feb) (Jury and Pathack, 1991; Jury et al., 1995). Winds originate from the Indian Winter Monsoon and Gulf of Oman moving southwest over the equatorial Indian Ocean as the Mascarene High retreats to the southwest in the austral summer (Fig. 1a). The mountains of eastern Madagascar block the prevailing easterlies (Barimalala et al., 2018), allowing the cyclonic Mozambique Channel Trough (MCT) to form in the Mozambique Channel (Barimalala et al., 2020). As a result, between 30° and 50°E the tropical rainbelt pushes down to 20°S in austral summer, following the centre of convergence rather than peak SSTs (Koseki and Bhatt, 2018), and is almost discontinuous from the tropical rainbelt to the east and west beyond the bounding meridional mountain ranges of the Great Rift Valley and the highlands of Madagascar (Koseki and Bhatt, 2018) (Fig. 1b).

In the north of the SEAfM region (northern Mozambique, northern Madagascar), incoming northeasterlies curve round to become northwesterlies (Fig. 1a) bringing monsoonal rainfall. Further south in the SEAfM region (both mainland southern Africa and Madagascar), moisture transport over both is driven by Tropical Temperate Troughs. Upper-level mid-latitude baroclinic instabilities combine with low-latitude moist convection to create a band of rainfall running northwest-southeast across southern Africa (Macron et al., 2014). The Mature and Late Phases of the Tropical Temperate Trough cycle influence rainfall across Madagascar (Macron et al., 2016). South of 25°S the moisture blocking influence of the mountains of Madagascar no longer exists, and rainfall in southeast Africa is derived from the southeasterly trade winds. While rainfall is still sufficiently seasonal to meet the criteria of monsoonal rain, there is no seasonal wind reversal (Fig. 1c).

Interannual variability: While peak regional SSTs are disconnected from convergence and rainfall, local SST variability still plays a role in the interannual variability of the MCT and therefore SEAfM and MSM rainfall amount (Barimalala et al., 2018). Stronger cyclonic conditions lead to stronger westerlies in the Mozambique Channel recurving winds, and therefore moisture transport away from Mozambique and onto Madagascar. This pattern leads to a rainfall dipole between Madagascar and southern Mozambique/South Africa. A stronger MCT is associated with a more southerly position of the ITCZ (Barimalala et al., 2020).

Unlike much of the circum-west Indian Ocean basin the Indian Ocean Dipole plays a weak role in MSM rainfall amount. The Indian Ocean Dipole is seasonally locked and, by definition, any atmospheric anomalies are terminated by the wind reversal at the onset of the austral monsoons. This is not to say that zonal processes are not important at other timescales or via other mechanisms such as

changing SSTs. While maximum interannual western Indian Ocean SST variability is between September and November before the onset of the MSM (Schott and McCreary Jr., 2001), these SST anomalies can persist and there is a statistically significant relationship between monthly SST and monthly rainfall in northern Madagascar in December ($r = 0.377$, $p = 0.021$) (Scroxton et al., 2017). At longer timescales MSM rainfall variability appears to respond to variability in SSTs and both zonal and meridional atmospheric circulation (Scroxton et al., 2017, 2019; Voarintsoa et al., 2019; Zinke et al., 2004). Subtropical SSTs may also play a role in regional rainfall, influenced by variability in the spatial teleconnections of El Niño-Southern Oscillation (Zinke et al., 2004).

3. Materials and methods

Anjohikely (15.56°S, 46.87°E) is a cave in the Narinda karst of northwest Madagascar. Sitting in Eocene limestone topped with dolomite, and 2.3 km SSW of the larger, well-documented Anjohibe, Anjohikely has 2.1 km of decorated passages, typically between collapsed dolines but with some well-decorated chambers with more restricted airflow (Laumanns et al., 1993). From Anjohikely, stalagmite AK1 was extracted in 2014. AK1 is a thin, 830 mm tall, candlestick-style, stalagmite (Fig. 2).

The age model for AK1 was determined from 20 U–Th ages (Table 1). U–Th samples weighing 15–25 mg were prepared and analysed at the Massachusetts Institute of Technology. Samples were combined with a ^{229}Th–^{233}U–^{236}U tracer, digested, purified via iron coprecipitation and ion exchange chromatography. U and Th were analysed on separate aliquots using a Nu Plasma II-ES multi-collector ICP-MS equipped with a CETAC Aridus II desolvating nebulizer. U–Th ages were calculated using the half-lives of 75,584 ± 110 for ^{230}Th, 245,620 ± 260 for ^{234}U (Cheng et al., 2013), 1.55125×10^{-10} yr^{-1} for ^{238}U (Jaffey et al., 1971) and an initial ^{230}Th/^{232}Th ratio of 4.4 (±2.2)x10^{-6}. One U–Th age at 322 mm was out of stratigraphic order with an anomalously old age. Low ^{238}U concentration (1140 ng/g) relative to bracketing ages (5780 and 4890 ng/g) is indicative of uranium loss, which would result in an anomalously old U–Th age. This age was removed from the age model.

The age model for AK1 was constructed using OxCal (Bronk Ramsey, 2008) using a P-Sequence Poisson process depositional model, with a k0 parameter of 0.1. Additional priors for suspected hiatuses were included at 707 mm and 760 mm. OxCal ran 2 million individual age model simulations. Replicating stalagmite ANJ94-5 from Anjohibe (Wang et al., 2019) was investigated using both the published StalAge age model and a newly constructed OxCal age model using the same depositional model and k0 parameter.

AK1 was sampled for stable isotopes (δ^{13}C and δ^{18}O) at increments ranging from 0.45 to 5 mm to achieve an approximately 5-year resolution (min: 15.3 years per sample, max: 0.7, average: 4.2, standard deviation 2.6) (Fig. 2). Lower sampling rate sections were drilled, and higher sampling rate sections were milled, both with a 1 mm diameter bit. A total of 645 samples were analysed for stable oxygen and carbon isotope ratios using a Thermo Scientific Gas Bench II for sample preparation and a Thermo Delta V Advantage isotope ratio mass spectrometer at the University of Massachusetts Amherst. Reproducibility of the standards is typically better than 0.04‰ for δ^{13}C and 0.06‰ for δ^{18}O (1σ).

Mineralogy was determined by x-ray diffraction (XRD) on ten samples using a PANalytical X'Pert PW1821 X-ray diffractometer at the University of Massachusetts Amherst. Samples were typically from U/Th sample holes at 14.5, 102, 284, 457.5, 631, 665, 700, 746.5 and 790 mm, plus an additional sample at 690 mm, just above a suspected hiatus.

4. Results

Stalagmite AK1 from Anjohikely grew from 5.22 to 2.00 kyr BP with hiatuses between 4.95 and 4.79 kyr BP and 4.31 and 3.93 kyr BP (Table 1, Fig. 3). Stalagmite growth is slower in the lower section of the stalagmite at between 0.1 and 0.2 mm/yr, and faster in the upper section of the stalagmite at 0.5 mm/yr, up to 1 mm/yr in places. The only carbonate mineral detected in all ten XRD measurements was aragonite, confirming visual observations of aragonite crystal morphology throughout the sample. The δ^{18}O record is relatively stable before 3.0 kyr BP, with 1–2‰ range in centennial scale variability (Fig. 2). A decrease in δ^{18}O between 3.0 and 2.5 kyr BP leads to two significant negative anomalies at 2.78 and 2.51 kyr BP before a return to the least negative δ^{18}O values at the cessation of growth at 2.00 kyr BP. To the first order we interpret stalagmite δ^{18}O in northwest Madagascar as a proxy for regional monsoonal strength, likely highly correlated to local rainfall amount, through a combination of the "amount effect" and strength of atmospheric convection (Scroxton et al., 2017; Voarintsoa et al., 2017, 2019; Wang et al., 2019). However, stalagmites rarely grow under 100% equilibrium conditions and the precise mechanisms controlling stalagmite δ^{18}O response to hydroclimate changes are discussed in section 5.2.

A positive δ^{18}O excursion at the top of stalagmite AK1 coincides with a reduction in stalagmite diameter and change in shape and location of the drip axis. Morphological changes are typically indicative of variable drip hydrology caused by changes in one or more of temperature, drip rate, calcium ion concentration or cave ventilation regime (Baker et al., 1998; Dreybrodt, 1999). This increases the likelihood of either non-equilibrium deposition and/or enhanced in-karst fractionation. As such, while the positive change in δ^{18}O in the top 99 mm of AK1 (younger than 2.40 kyr BP) is likely indicative of drying conditions, we suggest that the magnitude of δ^{18}O change is not directly comparable with the rest of the record.

At 707 mm, there is a growth hiatus between 4.31 and 3.93 kyr BP (±40 and ±35 yrs) (Fig. 4). The layer bounding surface has no truncated layers, a slight thinning of the stalagmite, an increase in δ^{18}O into the surface, and no obvious detrital material on the bounding surface. We interpret the layer bounding surface as Type L, one caused by decreased precipitation (Railsback et al., 2013). The hiatus is replicated in stalagmite ANJ94-5 from Anjohibe (Wang et al., 2019), ruling out cave or drip site specific drying in AK1 (section 5.1 for discussion). Replicated Type L hiatuses with positive isotope excursions indicate dry conditions and potentially the driest conditions of the mid/late Holocene. The 4.2 ka event therefore appears at least locally remarkable in northwest Madagascar. A dry anomaly is the opposite result to the wet conditions recorded at the 8.2 ka event (Voarintsoa et al., 2019) and what would be predicted from a North-Atlantic abrupt cold event.

A second Type L bounding surface occurs slightly above at 694 mm (3.78 kyr BP ±70yr). While the change in stalagmite colour and drip location is more substantial at this location, there is no significant isotopic change across this boundary, nor is there a noticeable change in growth rate. This layer may represent a short hiatus not resolvable within the current age model. A third Type L bounding surface occurs at 760 mm with a hiatus between 4.95 (±35yr) and 4.79 (±40yr) kyr BP.

The largest δ^{18}O excursions in the AK1 record are two negative (wet) anomalies at 2.78 (±0.03 kyr) and 2.51 kyr BP (±0.02 kyr) (Fig. 3). Both excursions are replicated, within dating errors, as dry events in the Dongge speleothem record at 2.75 and 2.50 kyr BP (Dykoski et al., 2005), while the earlier excursion is replicated in the Sanbao speleothem record (2.75 kyr BP) (Dong et al., 2010). The Huagapo speleothem record from Peru also contains a double dry excursion around this time, with peaks at 2.68 and 2.54 kyr BP

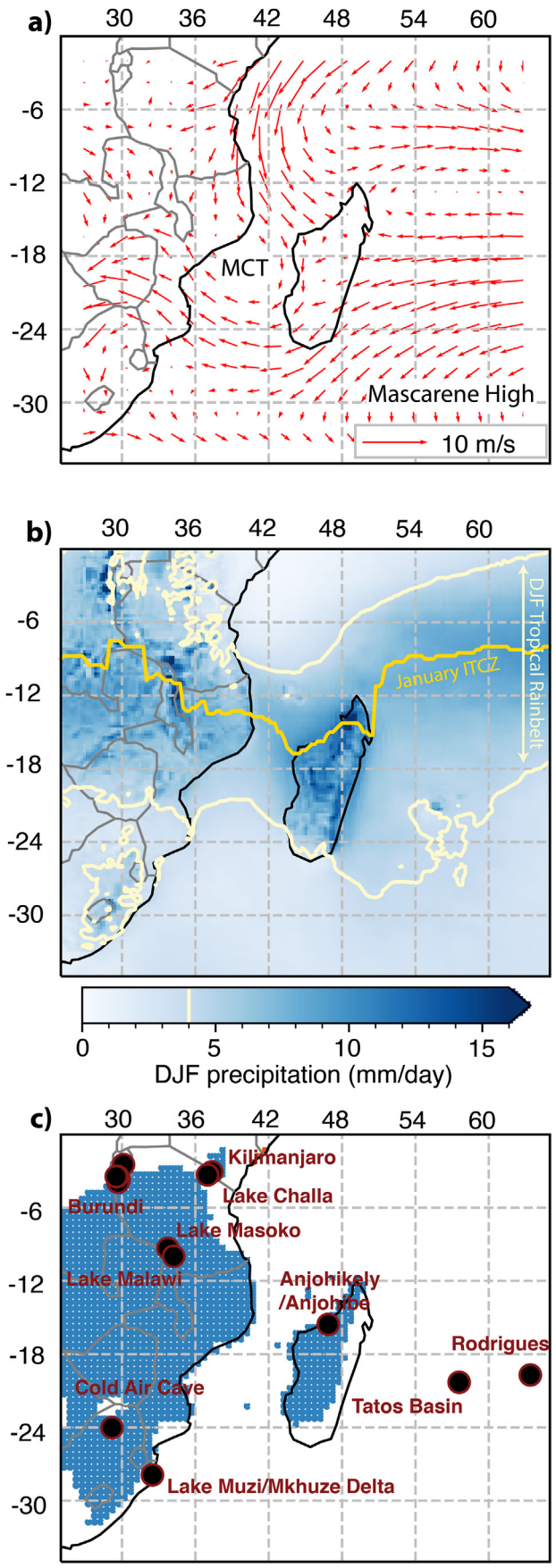

(Kanner et al., 2013) There is also a dry excursion in the Sahiya speleothem record of western India at 2.66 kyr BP (Kathayat et al., 2017) but the nearest U–Th age error of ±0.06 kyr does not allow direct 1:1 association with either event. These abrupt hydroclimate anomalies have received little attention despite being replicable in multiple monsoon-dominated tropical speleothem records, and with much greater magnitude there than more frequently studied Holocene climatic events such as the 4.2 ka event. Though not the focus of this paper, these climate anomalies are deserving of more thorough investigation in the future.

5. Discussion

5.1. Replication of stalagmites in northwest Madagascar at the Mid-Late holocene transition

Replication of results from the same or nearby caves is considered the gold standard for reliable climatic interpretation of stalagmite proxy time series (Dorale and Liu, 2009). Two speleothem $\delta^{18}O$ records from northwest Madagascar record the 5000 to 3000-year BP interval: AK1 from Anjohikely (this study) and ANJ94-5 from Anjohibe (Wang et al., 2019) (Fig. 5), 2.3 km northeast. Both have hiatuses close to the Mid- to LateHolocene transition. In AK1 the hiatus is at 4.31–3.93 kyr BP with age model uncertainty around ±40 years, and bracketing U–Th age uncertainty of ±26 and ± 34 years. In ANJ94-5 the hiatus is at 4.22–3.99 kyr BP, and while no age model uncertainty is provided, the nearest U–Th age uncertainty is ±30 and ±86 years. Both stalagmites have positive $\delta^{18}O$ excursions leading into the hiatus, and Type L bounding surfaces at the hiatus. This indicates the hiatus was caused by dry rather than wet conditions.

The 90-year offset in hiatus timing likely derives from the choice of age model. ANJ94-5 uses StalAge which has a constant growth rate bias. At the nearest U–Th age, the age model is 40 years younger than the analytical mean and outside the 2σ uncertainty (Fig. 5d). This suggests that the ANJ94-5 age model may underestimate the age of the hiatus. AK1 uses OxCal which has a mean growth rate bias when extrapolating beyond tie-points to hiatuses. This may result in a bias of the AK1 age model being 5 years too old at the hiatus. Recalculating the ANJ94-5 age model using OxCal gives a hiatus at 4.29–4.01 kyr BP (±49 and ±63 years). The hiatus occurs within error of the two stalagmite age models. Therefore, the primary result of this paper is replicated.

The timing of the hiatus may not be representative of the exact onset of drying. Hiatus timing will depend on hydrological response of a drip, including the size of the karst water store or the total surface area of rainwater catchment. The $\delta^{18}O$ records may provide further information. For example: ANJ94-5 shows a longer duration positive isotope excursion prior to the hiatus (2.4‰ over 1.6 mm or 96 years; OxCal age model suggests 67 years), likely due to the isotopic enrichment of a dwindling karst water store. Growth

Fig. 1. Location map of southwest Africa. a) ERA5 850 h Pa January mean wind direction and strength (red arrows) (Hersbach et al., 2019b). Approximate positions of the Mascarene High and Mozambique Channel Trough (MCT) are labelled. b) ERA5 DJF mean rainfall (blue gradient) (Hersbach et al., 2019a) with 4 mm isohyet (light yellow line) to denote approximate extent of the tropical rainbelt and January mean ERA5 Outgoing Longwave Radiation minima (yellow line) (Hersbach et al., 2019a) to denote approximate position of the summer ITCZ. c) Blue dots indicate the southern hemisphere summer monsoon regime, defined as where the summer (NDJAM) to winter (MJJAS) rainfall range is greater than 300 mm and Monsoon Precipitation Index (summer to winter range/annual precipitation) is greater than 0.5 (Wang and Ding, 2008). Black dots with red edges indicate locations of paleoclimate records. ERA5 data (Hersbach et al., 2020) was accessed through the Copernicus Climate Data Store. (For interpretation of the references to colour in this figure legend, the reader is referred to the Web version of this article.)

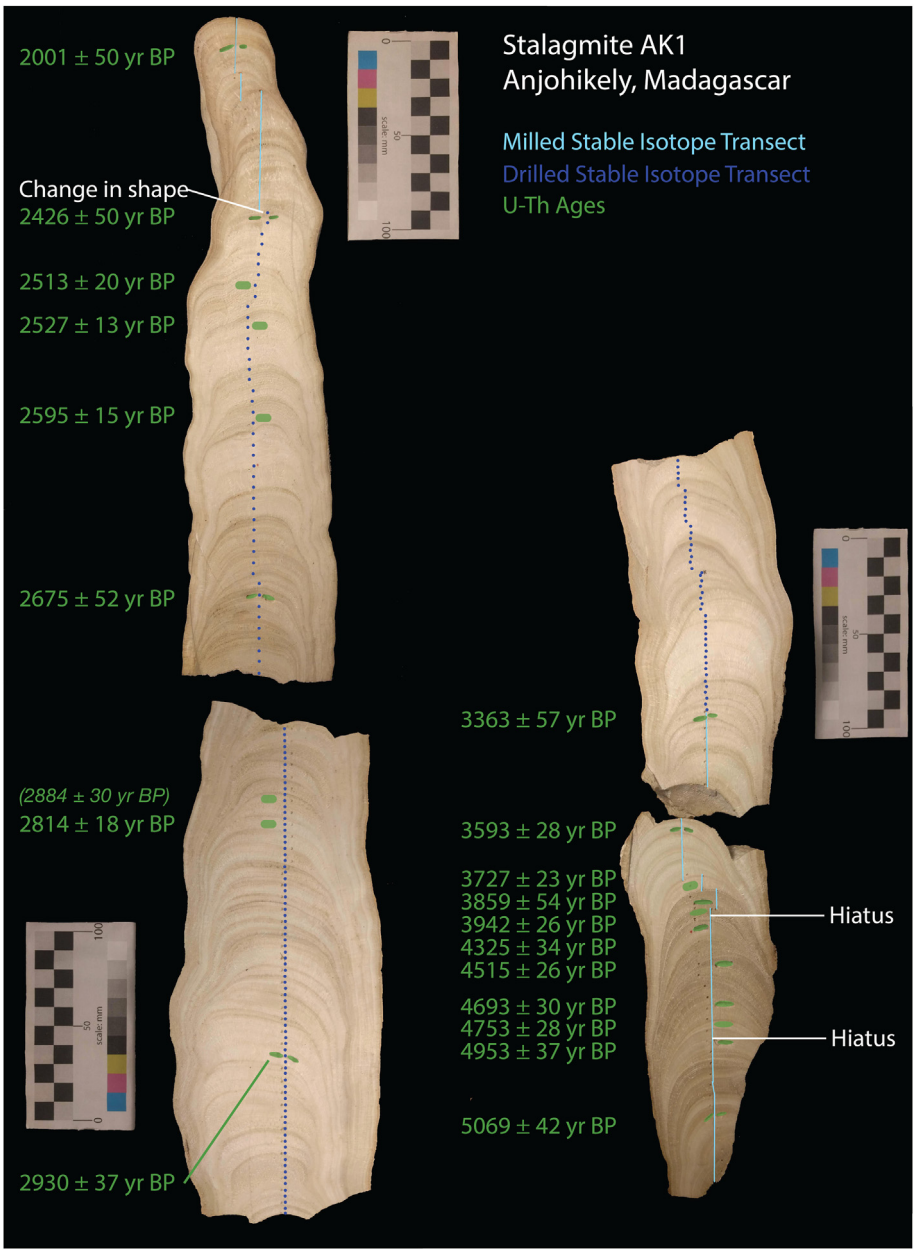

Fig. 2. Photographs of stalagmite AK1 with scalebar length of 100 mm. Green shading denotes U–Th sampling locations, dark blue dots show stable isotope drill holes, light blue lines show stable isotope milling trench. (For interpretation of the references to colour in this figure legend, the reader is referred to the Web version of this article.)

of AK1 terminates quickly with minor isotopic enrichment before the hiatus (0.7‰ over 1.5 mm or 14 years).

In the long term, both stalagmites record negative excursions between 4.6 and 4.5 kyr BP indicating wetter conditions, and both show positive excursions, indicating drying from ~4.5 kyr BP onwards. The local $\delta^{18}O$ minimum prior to substantial drying is at 4.32 kyr BP in AK1 (age model error of ±35 years). In ANJ94-5 an equivalent isotopic shift is either a $\delta^{18}O$ minimum at 4.34 kyr BP years (OxCal: 4.39kyr BP, age model error of ±46 years) or an abrupt $\delta^{18}O$ change at 4.30 years (OxCal: 4.35kyr BP, age model error of ±31 years). Therefore, while the onset of the growth hiatus in both stalagmites is synchronous (within error) with the 4.2 ka event, the $\delta^{18}O$ records suggest that gradual drying began at ~4.5 kyr BP, and rapid drying at ~4.3 kyr BP, before the 4.2 ka event.

5.2. Replication of stalagmites in northwest Madagascar of Mid- & Late- Holocene climate

Elsewhere, the $\delta^{18}O$ records of speleothems ANJ94-5 and AK1 do not overlie each other and do not initially appear to replicate. However, cave conditions, drip-pathway contributions, stalagmite mineralogy and other hydroclimate indicators such as growth rate may explain some of the discrepancies. ANJ94-5 is a mixed mineralogy stalagmite, whereas AK1 is aragonite. The aragonite sections of ANJ94-5 at 4.8–4.6 kyr BP and 4.0 kyr BP onwards have $\delta^{18}O$ values comparable to those of AK1. However, the isotopic difference between calcite and aragonite sections of ANJ94-5 of ~2‰ is far larger than the expected offset between calcite and aragonite of ~0.8‰ determined from laboratory studies (Kim et al., 2007), theoretical calculations (Tarutani et al., 1969), and in

Table 1
U–Th dating table for stalagmite AK1.

Sample ID	Depth	^{238}U	± (2σ)	^{232}Th	± (2σ)	δ^{234}U	± (2σ)	(^{230}Th/^{238}U)	± (2σ)	^{230}Th/^{232}Th	± (2σ)	Age (yr)	± (2σ)	Age (yr)	± (2σ)	δ^{234}U initial	± (2σ)	Age (yr BP)	± (2σ)
	(mm)	(ng/g)[a]		(pg/g)[a]		(per mil)[b]		activity		ppm atomic		(uncorr)[c]		(corr)[d]		(per mil)[e]		(corr)[f]	
AK1-15	14.5	5200	100	2708	57	−3.5	1.5	0.01883	0.00045	574	14	2081	50	2066.4	9.5	−3.6	1.5	2001	50
AK1-99	102	5070	100	1452	34	−2.4	1.5	0.02260	0.00044	1250	29	2499	50	2491.4	8.4	−2.4	1.5	2426	50
AK1-A (138)	138	7260	150	399	9	−3.5	4.7	0.02330	0.00014	6740	71	2580	20	2578.2	20.2	−3.5	4.8	2513	20
AK1-B (160)	160	7700	150	228	6	−4.9	2.1	0.02339	0.00010	12,500	190	2593	13	2592.2	12.8	−4.9	2.1	2527	13
AK1-C (206)	206	4820	97	578	12	−4.4	2.0	0.02402	0.00013	3180	23	2663	15	2659.6	15.4	−4.4	2.1	2595	15
AK1-275	284	4890	98	922	26	−3.3	1.4	0.02477	0.00046	2080	56	2745	52	2739.5	8.2	−3.3	1.4	2675	52
*AK1-D (322)**	*322*	*1140*	*23*	*833*	*17*	*−6.5*	*2.7*	*0.02671*	*0.00024*	*578*	*6*	*2972*	*28*	*2949.3*	*30.1*	*−6.5*	*2.7*	*2884*	*30*
AK1-E (335)	335	5780	120	481	10	−5.6	2.2	0.02594	0.00015	4950	48	2882	18	2879.5	18.	−5.7	2.2	2814	18
AK1-450	457.5	6480	130	272	17	−1.3	1.3	0.02706	0.00033	10,200	640	2996	37	2994.6	8.1	−1.3	1.3	2930	37
AK1-625	631	4580	92	287	19	−1.1	1.3	0.03093	0.00050	7840	510	3429	57	3427.8	9.1	−1.1	1.3	3363	57
AK1-665	665	3200	64	197	16	−2.0	2.2	0.03298	0.00023	8510	680	3664	28	3662.1	27.8	−2.0	2.3	3593	28
AK1-F (691)	691	3870	77	187	5	−4.6	2.4	0.03403	0.00018	11,200	220	3793	23	3791.7	22.6	−4.6	2.4	3727	23
AK1-693	700	2980	60	1804	49	−4.2	2.1	0.03539	0.00046	928	21	3946	53	3927.7	53.9	−4.3	2.1	3859	54
AK1-G (714)	703	2960	59	532	11	−2.5	2.4	0.03604	0.00021	3190	32	4013	26	4007.4	26.2	−2.6	2.4	3942	26
AK1-710	710.5	2950	59	364	19	−3.3	2.2	0.03940	0.00028	5080	240	4398	34	4394.5	33.9	−3.4	2.2	4325	34
AK1-727	727.5	4130	83	563	20	−2.6	1.9	0.04110	0.00021	4790	140	4589	25	4584.7	25.5	−2.6	1.9	4515	26
AK1-746	746.5	3560	71	477	18	−0.8	2.0	0.04274	0.00025	5060	170	4766	30	4762.3	30.2	−0.8	2.0	4693	30
AK1-H (756)	756	4300	86	450	10	−4.0	2.4	0.04307	0.00022	6540	62	4821	28	4817.9	27.8	−4.1	2.5	4753	28
AK1-761	761.5	4090	82	2191	47	−5.2	1.9	0.04492	0.00030	1330	13	5039	36	5022.5	36.9	−5.2	1.9	4953	37
AK1-763	790	7130	140	1076	28	0.5	1.2	0.04605	0.00037	4850	92	5138	42	5133.9	13.	0.5	1.2	5069	42

[a] Reported errors for ^{238}U and ^{232}Th concentrations are estimated to be ±1% due to uncertainties in spike concentration; analytical uncertainties are smaller.
[b] $\delta 234U = ([^{234}U/^{238}U]_{activity} - 1) \times 1000$.
[c] $[^{230}Th/^{238}U]_{activity} = 1 - e^{-\lambda 230 T} + (\delta^{234}U_{measured}/1000)[\lambda_{230}/(\lambda_{230} - \lambda_{234})](1 - e^{-(\lambda 230 - \lambda 234)T})$, where T is the age. "Uncorrected" indicates that no correction has been made for initial ^{230}Th.
[d] Ages are corrected for detrital ^{230}Th assuming an initial ^{230}Th/^{232}Th of $(4.4 \pm 2.2) \times 10^{-6}$.
[e] δ234Uinitial corrected was calculated based on ^{230}Th age (T), i.e., $\delta^{234}U_{initial} = \delta^{234}U_{measured} \times e^{\lambda 234 \times T}$, and T is corrected age.
[f] B.P. stands for "Before Present" where the "Present" is defined as the January 1, 1950 C.E.

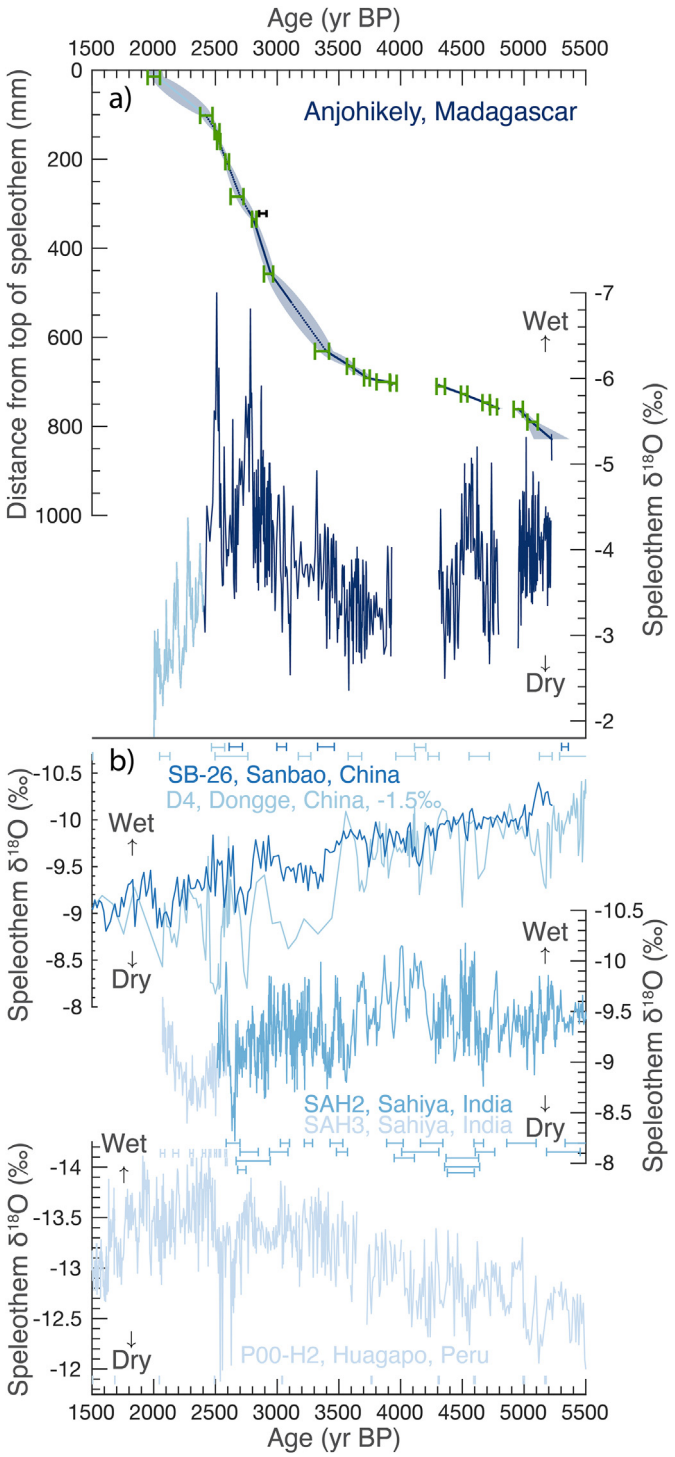

Fig. 3. a) Results from stalagmite AK1 from Anjohikely, northwest Madagascar, showing top: U–Th ages (green error bars), OxCal age model (blue lines) and associated 95% confidence interval (blue shading), and bottom: stalagmite $\delta^{18}O$. Data from the top 99 mm are shown in a lighter blue. b) comparison with other monsoon influenced speleothem $\delta^{18}O$ records. From top to bottom: Sanbao and Dongge caves in China (Dong et al., 2010; Dykoski et al., 2005), Sahiya cave in India (Kathayat et al., 2017) and Huagapo cave in Peru (Kanner et al., 2013). (For interpretation of the references to colour in this figure legend, the reader is referred to the Web version of this article.)

stalagmites from Anjohibe (Scroxton et al., 2017).

Some discrepancies between the $\delta^{18}O$ records could be explained by differences in cave conditions. ANJ94-5 was collected from a chamber open to the atmosphere, with atmospheric CO_2 concentrations (Wang et al., 2019). ANJ94-5 was therefore likely subject to (relatively) more kinetic fractionation through rapid degassing and a (relatively) larger extent of disequilibrium fractionation during precipitation (Mickler et al., 2006). Anjohikely has more restricted chambers and a greater areal coverage of precipitated calcite, especially on the walls and floor. Therefore, while additional evidence from ANJ94-5 suggests that isotopic variability may still be climatic in origin (Wang et al., 2019), the absolute $\delta^{18}O$ values are likely not comparable with AK1, sourced from a more restricted chamber in a 'wetter' cave.

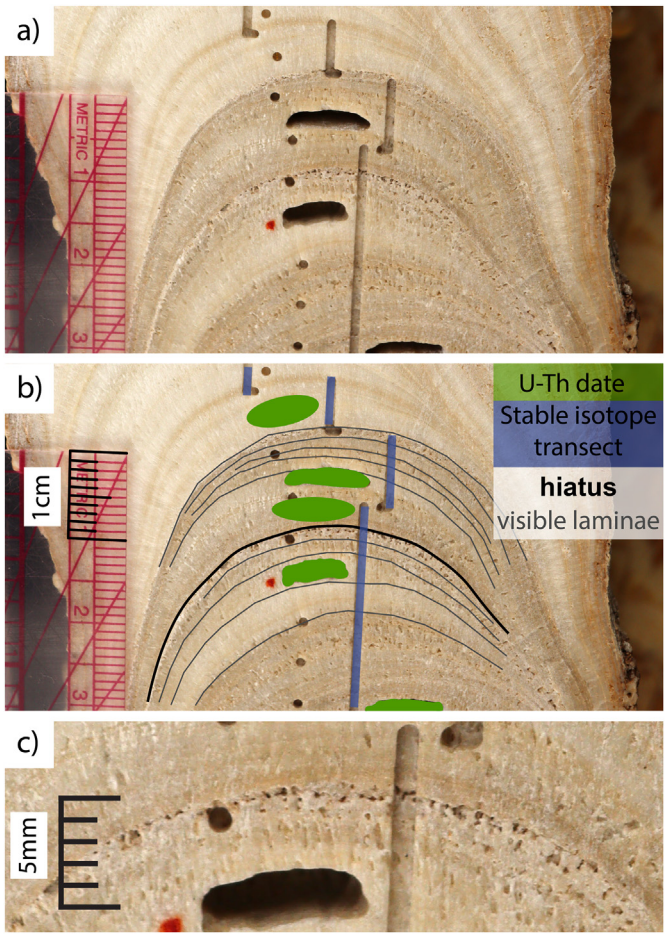

Fig. 4. Close-up of the Mid- to Late-Holocene hiatus in AK1. a) image with no annotation. b) image with annotation. Green shaded areas denote U–Th date sampling locations, blue shaded areas denote stable isotope transect trench, visible laminae in thin black lines, the Mid- to Late-Holocene hiatus in thick black line, unmarked circular pits are stable isotope drill holes from a low-resolution pilot study. c) higher zoom unannotated image of the Mid- to Late-Holocene hiatus.

However, as ANJ94-5 oxygen isotope values are frequently lower than AK1, even during periods of identical mineralogy, there must be additional drip pathway contributions that contribute to different isotopic responses in the two stalagmites. For example, differences in storage and mixing and in-karst evaporation during the dry season (Markowska et al., 2020) might lead to different sensitivities to different parts of the hydrologic system: for example extreme events or seasonal vs long-term mean.

With these caveats in mind, a comparison of centennial scale positive and negative periods of $\delta^{18}O$ in both stalagmites does show good reproducibility and can be interpreted as broad-scale climatic changes in the hydrological cycle. Both stalagmites show a gradual

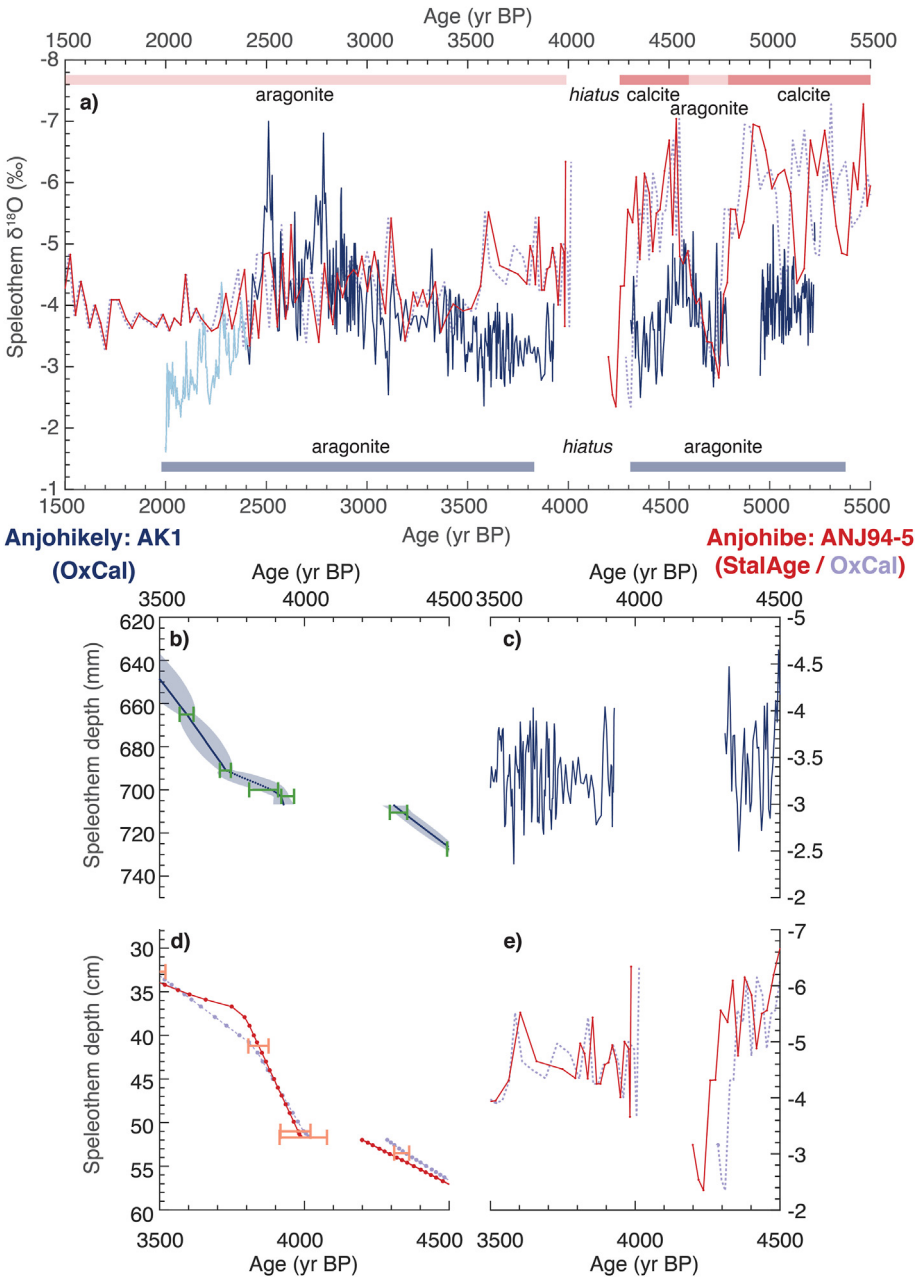

Fig. 5. Comparison of speleothems from Anjohikely (AK1, blue colours, this study, OxCal age model) and Anjohibe (ANJ94-5, red colours: original StalAge model (Wang et al., 2019), purple line: OxCal age model, this study), two caves 2 km apart in northwest Madagascar. a) speleothem $\delta^{18}O$ during the period of overlap. b-e) 1000-year close-up of events around the 4.2 ka BP event indicating the contemporaneous hiatus in both speleothems. b,d) Age depth model, circles indicate individual stable isotope data points linked by line. Shading denotes 2σ age model error for stalagmite AK1. Light coloured error bars show individual dates with 2σ error. c,e) individual $\delta^{18}O$ measurements for each stalagmite.

positive (drying) trend between 5.5 and 4.3 kyr BP with modest centennial scale variability indicated by more negative $\delta^{18}O$ values (wetter) between, 5.15 and 4.95 kyr BP, and around 4.5 kyr BP, and more positive $\delta^{18}O$ values (drier) between 4.8 and 4.65 kyr BP, and 4.5 and 4.3 kyr BP.

After (above) the hiatus there is agreement between the growth rate of ANJ94-5 and the isotopes of AK1. Between 3.15 and 2.5 kyr BP there is a 0.7‰ $\delta^{18}O$ decrease in AK1, suggesting wetter conditions (3.5–3.15 kyr BP: 3.7‰, 3.15 to 2.4 kyr BP: 4.4‰). ANJ94-5 also has a negative $\delta^{18}O$ excursion, but it is half the size at around 0.35‰ (3.5–3.15 kyr BP: 3.95‰, 3.15 to 2.4 kyr BP: 4.3‰). An increased growth rate in ANJ94-5 is also likely indicative of wetter conditions, either through greater transport of calcium ions by reduced prior calcite precipitation or enhanced flow rate, or by enhanced vegetative activity increasing soil pCO_2 and the dissolution of the karst host rock. The abrupt negative excursion in AK1 at 2.51 kyr BP does appear to have some expression in ANJ94-5, albeit muted, but the 2.78 kyr BP excursion is less clear.

Both stalagmites return to higher $\delta^{18}O$ (drier conditions) at 2.4 kyr BP. AK1 increases from −4.4‰, between 3.15 and 2.4 kyr BP to −3.0‰ between 2.4 and 2.0 kyr BP. ANJ94-5 increases from −4.3‰, between 3.15 and 2.4 kyr BP to −3.9‰ between 2.4 and 2.0 kyr BP. Coincident with this isotopic change in AK1 is a shape change, with the stalagmite becoming thinner and less cylindrical. We suggest that from 2.4 kyr BP onwards, AK1 may also be subject to enhanced disequilibrium effects, perhaps related to

changes in cave ventilation regime, and/or a progressive drying of the drip prior to the termination of growth. We suggest that the isotopic values during this section (younger than 2.4 kyr BP) are not directly comparable to those elsewhere in the stalagmite.

The consequences of different cave conditions, karst storage and drip pathways on stalagmite $\delta^{18}O$ remains a working hypothesis. Valuable cave monitoring efforts in the area are still in their infancy (Voarintsoa et al., 2021) but already highlight how cave ventilation may be an important intra-site control on speleothem $\delta^{18}O$. More efforts are needed focusing on replicating northwest Madagascar speleothem $\delta^{18}O$ and understanding the local hydrology at cave and drip level. Despite numerous environmental controls on exact speleothem $\delta^{18}O$ values (as is likely the case for all stalagmite paleoclimate records), the majority of controls influence $\delta^{18}O$ in the same direction (wetter conditions tend to negative $\delta^{18}O$). A first order interpretation of AK1 $\delta^{18}O$ variability being negatively correlated with monsoon strength and precipitation amount still holds.

5.3. Regional variability in the African monsoons

Here we explore hydroclimate variability across the Mid- to Late- Holocene transition in the broader southeast Africa region (Figs. 6 and 7). In the southern hemisphere of East Africa, the Kilimanjaro ice core $\delta^{18}O$ shows a gradual drying from 4.5 kyr BP, accelerating at 3.65 kyr BP (Thompson et al., 2002) (Fig. 6a). An increase in dust occurs at 4.2 kyr BP but oxygen isotopes indicate only a gradual change from warmer and wetter conditions to dry and cooler. A pollen-based estimate of precipitation from multiple sites in Burundi suggests a transition from relatively stable conditions to higher-amplitude swings between low and high precipitation around 3.6 kyr BP, but no abrupt 4.2 ka event (Bonnefille and Chalie, 2000) (Fig. 6b). Records from Lake Challa show conflicting changes in low resolution records that may not have the resolution to record an abrupt 4.2 ka event (Fig. 6c and d). The BIT record shows a peak in wet conditions between 4.2 and 3.7 kyr BP, but this is part of a long-term millennial scale trend lasting 1.5 kyr (Verschuren et al., 2009). The leaf wax δD is inverse, indicating peak dry conditions between 4.2 and 3.7 kyr BP, again part of a longer millennial scale trend. The authors reconcile these differences suggesting that the δD likely records moisture transport processes rather than local rainfall amount (Tierney et al., 2011), and attribute changes to tropical zonal reorganisation.

Further south in the SEAfM, at Lake Masoko, magnetic susceptibility data indicates drying begins around 4.6 kyr BP, peaking around 4.4 kyr BP (Garcin et al., 2006) (nearest calibrated radiocarbon age error around ±250 years 2σ (Gibert et al., 2002)) (Fig. 6e). A possible short hiatus occurs between 4.0 and 3.9 kyr BP. At Lake Malawi, the biogenic silica mass accumulation rate indicates drying begins around 4.65 kyr BP (nearest calibrated radiocarbon age error ±130 years 2σ (Johnson et al., 2002)) (Fig. 6f). Between 4.4 and 3.95 kyr BP there is only a single datapoint, which given surrounding deposition rates, we interpret as an interpolated point through an unrecognised hiatus.

In the Indian Ocean pollen counts (specifically ln (*Latania*/*Eugenia*)) from the Tatos Basin in Mauritius suggest drier conditions between 4.5 and 4.1 kyr BP (nearest uncalibrated radiocarbon age error ±70 years 2σ), while sediment core ln (Ca/Ti) ratios indicate brief centennial wet events at 4.38 and 4.15 kyr BP, all on a background shift from wetter to drier conditions from 4.8 kyr BP (de Boer et al., 2014) (Fig. 6j). Further east on Rodrigues, speleothem $\delta^{18}O$ values from La Vierge show no change in conditions at the 4.2 ka event but do show a gradual drying beginning around 3.9 kyr, interpreted as part of the widespread tropical climatic changes at this time (Li et al., 2018) (Fig. 6i).

In South Africa, there is little change in speleothem T8 $\delta^{18}O$ at Cold Air Cave (Holmgren et al., 2003), with slightly wetter conditions between 4.6 and 4.05 kyr BP and slightly dry conditions between 4.05 and 3.8 kyr BP (Fig. 6l). A growth phase of stalagmite T5 between 4.4 and 3.95 kyr BP suggests wetter conditions during the Middle to Late Holocene transition but could be a coincident change in drip hydrology (Fig. 6k). The nearest U–Th age error is ±150 years 2σ (Repinski et al., 1999). Sediment core x-ray fluorescence determined Ca/K from Lake Muzi (Humphries et al., 2019) (Fig. 6m) and Sr/Al from Mkhuze Delta (Humphries et al., 2020) (Fig. 6n) in eastern South Africa both indicate periods of wet conditions between 4.25 and 3.8 kyr BP. The nearest calibrated radiocarbon age error at Lake Muzi is ±130 years 2σ (Humphries et al., 2019) and the nearest calibrated radiocarbon age error at Mkhuze Delta is ±87 years (contributing 76.9% of the 2σ probability range) (Humphries et al., 2020).

5.4. Age uncertainty, timing, and coherence with the 4.2 ka event

A hydroclimate event at the Mid- to Late-Holocene transition appears to have some local significance in the SEAfM domain with peak anomalies of several records within the age uncertainty of the 4.2 ka event (4.26–3.97 kyr BP). Peak dry conditions occur between 4.5 and 4.1 kyr BP at Lake Masoko (~±250 years 2σ), 4.4–4.0 kyr BP at Lake Malawi (~±130 years 2σ), 4.2–4.0 kyr BP at Anjohibe (nearest U–Th age error ±30 years 2σ), 4.3–3.9 kyr BP at Anjohikely (age model error ±60 years 2σ, nearest U–Th age error ±34 years 2σ), and 4.5–4.1 kyr BP at Tatos Basin (~±70 years 2σ). Peak wet conditions occur at 4.2–3.8 kyr BP at Lake Muzi (~±130 years 2σ) and 4.2–3.9 kyr BP (~±87 years 2σ) at Mkuze Delta. Records with smaller age uncertainty show onsets closer to the 4.26 kyr BP onset of the 4.2 ka event. However, the signal appears geographically limited, with little or no signal seen at Burundi, Kilimanjaro and Lake Challa in the north and Rodrigues in the east. The Cold Air Cave records from South Africa are inconclusive.

Many of the regional paleoclimate records summarised above have relatively low and/or variable resolution, have considerable age uncertainty, and are without published age model uncertainties/envelopes. Therefore, while peak anomalies of the Mid- to Late-Holocene transition in the SEAfM region appear to overlap within age uncertainty of the 4.2 ka event, the age uncertainties prevent a causal relationship being automatically inferred. An age-model-uncertainty-resolved-test of synchronicity is beyond the scope of these records and this paper. In a companion paper in this issue Scroxton et al. (2022) synthesise other high resolution, precisely dated records with publicly archived interpolated age uncertainty data from the wider circum-Indian Ocean basin region and use age uncertainty resolved principal component analysis to assess the coherency of change. In this SEAfM focused study we proceed with the stated ages in the original publications which, given the close to Gaussian nature of age uncertainty, remain the most likely ages.

In particular, we note that the hydroclimate anomalies frequently begin around 4.5 kyr BP, or earlier, and that change is often gradual. In Anjohikely and Anjohibe gradual drying begins around 4.5 kyr BP with more abrupt drying at 4.3 kyr BP (section 5.1). This result occurs elsewhere in the SEAfM region. Drying begins around 4.6 kyr BP at Lake Masoko, Lake Malawi, and the Tatos Basin. Wet conditions begin around 4.6 kyr BP at the Mkhuze Delta. This is consistently earlier and more gradual than the abrupt 4.26 kyr BP onset of the 4.2 ka event in the Mediterranean and Middle East. Further, a 4.6 kyr BP hydrological change may have a stronger regional coherence, with the Lake Challa and Kilimanjaro records also potentially showing change at this time. Therefore, the observed climate anomalies at the Mid-to Late-Holocene transition

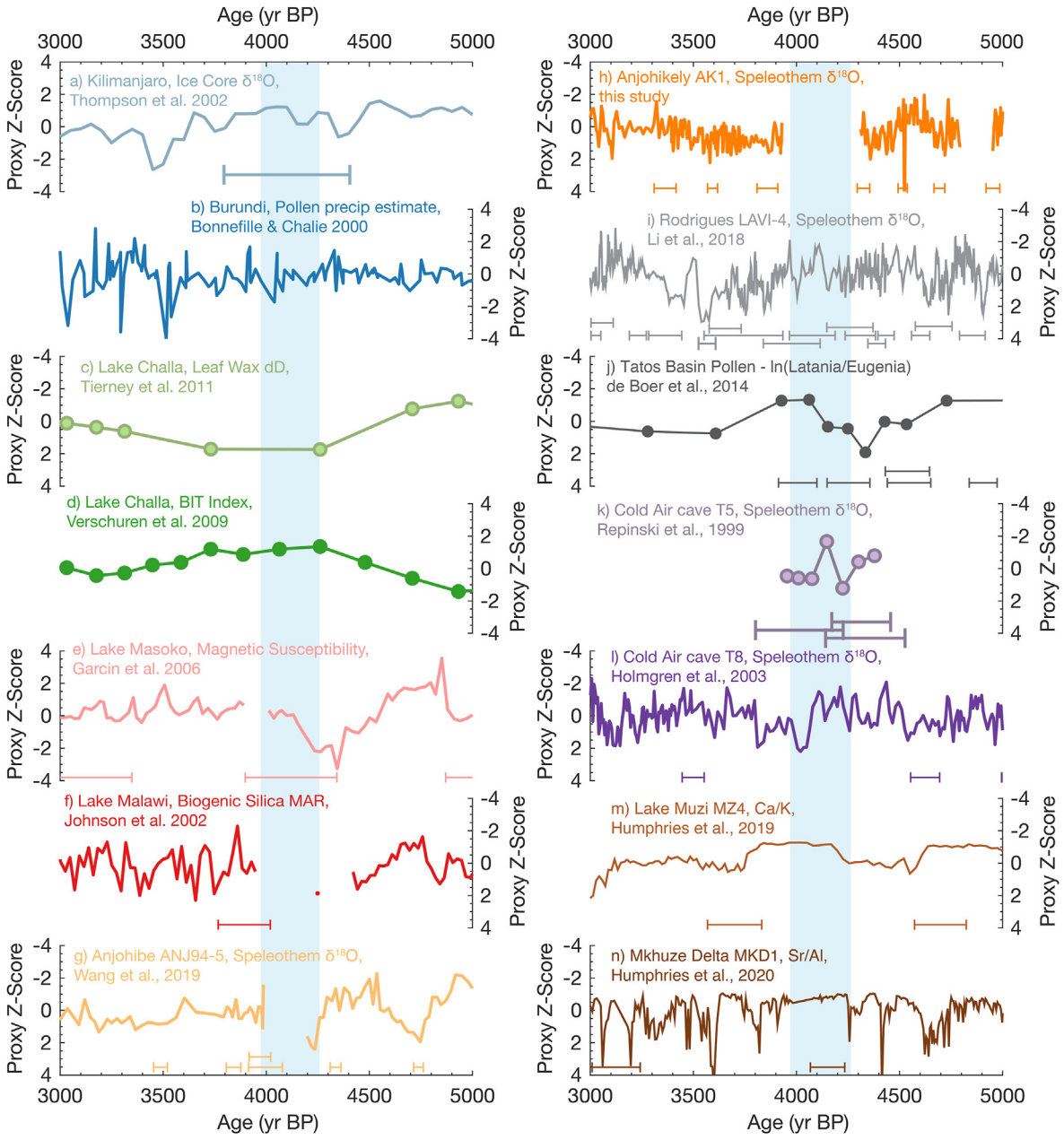

Fig. 6. Regional hydroclimate changes in southeast Africa between 5 and 3 kyr BP. For each record proxy z-score is calculated between 2.5 and 5.5 kyr BP to reduce the influence of orbital scale changes. Circles indicate datapoints. Lines without circles are at higher resolution so circles have been omitted for clarity. Error bars show radiocarbon or U–Th dates for each record and errors. Blue bars indicate the duration of the 4.2 ka event. Records are plotted so that wet conditions are consistently up.

in the SEAfM domain may not be forced by the 4.2 ka event, and instead be part of a lower frequency regional change. If present, the 4.2 ka event appears to act on top of this regional climate variability, in the same direction, and may have a more localised impact.

5.5. Spatial pattern of a Mid- to Late-holocene regional hydroclimate anomaly

The spatial pattern of peak hydroclimate anomalies at the Mid- to Late-Holocene transition (not necessarily related to the 4.2 ka event) approximates the spatial pattern of hydroclimate anomalies during weak MCT years (Fig. 7a). Some local mismatches occur at Cold Air Cave, and possibly Rodrigues, Lake Muzi and Mkhuze Delta. In the modern climate, weak MCT years (1981, 1990, 2006, 2017) result in dry conditions in northern Mozambique, Madagascar and Mauritius, wet conditions over South Africa, weakly dry conditions over Malawi and weakly wet conditions over Burundi and Tanzania (Barimalala et al., 2020; Xie and Arkin, 1997). This suggests that the Mid- to Late-Holocene transition may be locally expressed as a period of more frequent weak MCT events. Further comparison with ERA-Interim reanalysis of the 850 hPa specific humidity (Fig. 7b) shows a similar pattern, indicating the rainfall anomalies are associated with decreased moisture convergence over the northern Mozambique channel (Barimalala et al., 2020; Dee et al., 2011). Modern SST anomalies suggest decreased rainfall is associated with higher subtropical SSTs southeast of Madagascar, and cooler tropical SSTs northeast of Madagascar (Barimalala et al., 2020). Paleo-SSTs in the Mozambique Channel

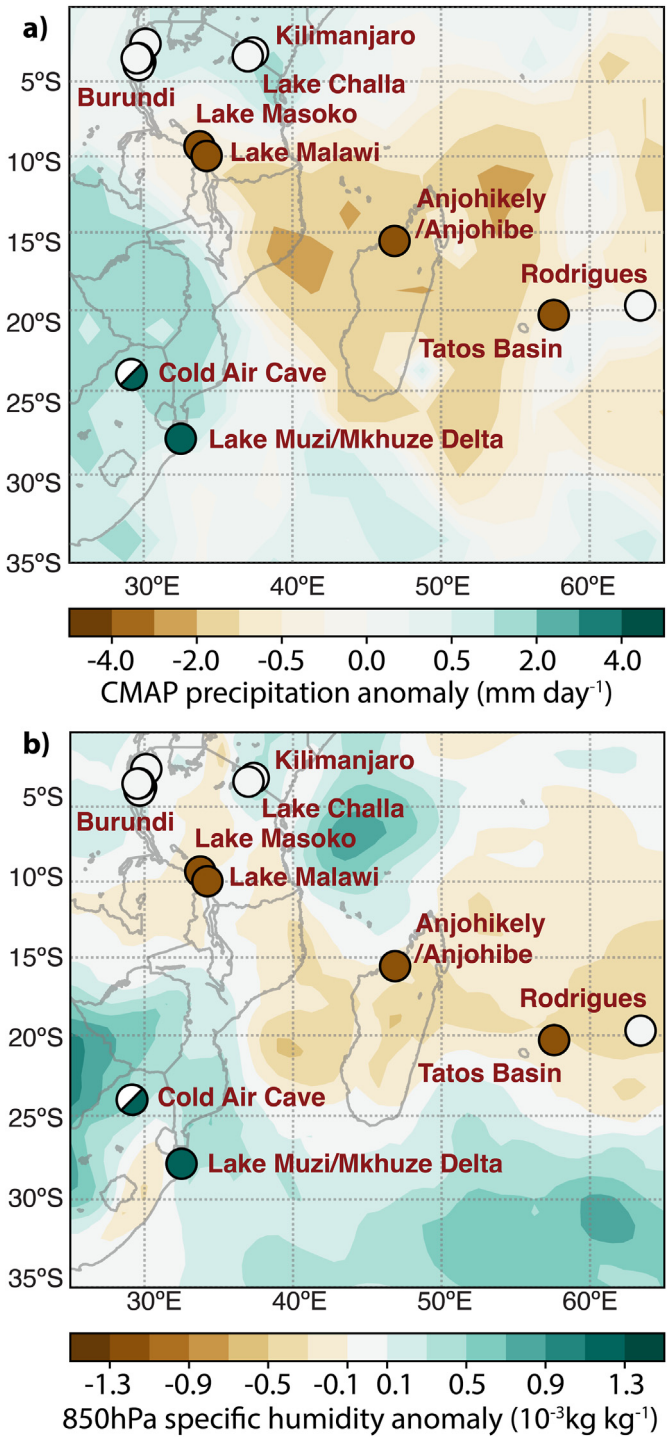

Fig. 7. Combined modern and paleo-climate anomaly maps. Coloured circles indicate wet (green), dry (brown) or no (white) anomaly determined from paleoclimate records during the 4.2 ka event at individual sites. Evidence from Cold Air Cave is inconclusive and shows two colours. Map colours indicate a) CMAP precipitation anomaly (Xie and Arkin, 1997; Xie and Arkin, 1997) and b) ERA-Interim (1980–2017) reanalysis specific humidity anomaly at 850 h Pa (Dee et al., 2011) for weak Mozambique Channel Trough years: 1981, 1990, 2006, 2017. Figures based on (Barimalala et al., 2020).

show a slight but non-significant cooling (Weldeab et al., 2014).

We suggest the regional hydroclimate anomaly at the Mid- to Late-Holocene transition is associated with a period of more frequent weak MCT events, where reduced cyclonic conditions, atmospheric convergence and recurving of moisture-bearing winds over the Mozambique Channel and onto Madagascar leads to reduced rainfall in the MSM. Weak MCT years are associated with a northerly location of the summer ITCZ relative to its climatological mean in the west Indian Ocean (Barimalala et al., 2020). Therefore, we hypothesise that the austral summer ITCZ over the western Indian Ocean was further north during the Mid- to Late-Holocene transition.

5.6. Comparison with the 8.2 ka event

The 4.2 ka event is often considered a smaller version of the 8.2 ka event (Bond, 1997). The 8.2 ka event is an abrupt North Atlantic cooling episode likely caused by the release of meltwater from glacial lakes Agassiz and Ojibway into the North Atlantic and subsequent reduction in North Atlantic Deepwater formation (Alley et al., 1997; Alley and Ágústsdóttir, 2005; Barber et al., 1999; Brouard et al., 2021). The resulting climate anomaly is seen throughout the globe (Morrill et al., 2013; Parker and Harrison, 2022). Drying is reported in equatorial eastern Africa at Kilimanjaro (Thompson et al., 2002) and offshore of the Tanzanian coast (Liu et al., 2017). In the SEAfM region wet anomalies are observed in the Burundi pollen precipitation estimate (Bonnefille and Chalie, 2000), Lake Challa leaf wax δD (Tierney et al., 2011), Lake Chilwa (Thomas et al., 2009), Anjohibe (Duan et al., 2021; Voarintsoa et al., 2019), Cold Air Cave (Holmgren et al., 2003) and the Mafadi Wetlands in Lesotho (Fitchett et al., 2017). There does not appear to be major hydroclimate anomalies at Lake Masoko (Garcin et al., 2006) or Lake Malawi (Castañeda et al., 2007; Johnson et al., 2002). This pattern indicates a more regionally coherent wetting, consistent with an enhanced SEAfM and southerly excursion of the austral summer tropical rainbelt (Voarintsoa et al., 2019). This result is in contrast to peak hydroclimate anomalies at the Mid- to Late-Holocene where drying is observed at Anjohikely, Anjohibe, Lake Malawi and Lake Masoko, wetting at Lake Muzi and the Mzhuze Delta, and more muted responses elsewhere (Fig. 7). This casts doubt as to whether 1) hydroclimate anomalies at the Mid- to Late-Holocene boundary in the region are an expression of the 4.2 ka event and/or 2) that the 4.2 ka event likely had a very different climate mechanism, especially given the absence of a North Atlantic freshwater anomaly (Bradley and Bakke, 2019).

5.7. The 4 kyr tropical climate shift in the MSM

Finally, it is worth noting that there is an isotopic offset between the latest Middle Holocene and the start of the Late Holocene in both AK1 and ANJ94-5. If this isotopic shift is climatic, and not related to non-climatic changes in drip hydrology at the hiatuses, then the change is likely evidence of an expression of the 4 kyr tropical climate shift i (Denniston et al., 2013; Gagan et al., 2004; Giosan et al., 2018; Li et al., 2018; MacDonald, 2011; Toth and Aronson, 2019; Scroxton et al., 2022) in the MSM. The 4 kyr tropical climate shift can be distinguished from the 4.2 ka event here by anomaly shape (the 4.2 ka event is transient between 4.26 and 3.97 kyr BP, while the 4 kyr tropical climate shift is longer lasting (Scroxton et al., 2022)) but continually growing stalagmites are required to test the timing of the 4 kyr climate shift in the MSM and synchronicity with wider Indian Ocean basin hydroclimate.

6. Conclusions

Stalagmites from Anjohibe (Wang et al., 2019) and Anjohikely (this study) show replicated Type L bounding surface hiatuses, with abrupt drying beginning near 4.3 kyr BP, indicating likely dry conditions in northwest Madagascar at the Mid- to Late-Holocene transition. The response on Madagascar is opposite to the local

response to the 8.2 ka event (Voarintsoa et al., 2019) suggesting a fundamentally different climate mechanism and lending weight to the idea that the 4.2 ka event was not forced by a North Atlantic freshwater pulse.

Regionally, coincident dry conditions at Lake Masoko and Lake Malawi provides evidence for a significant hydroclimate anomaly at the Mid- to Late-Holocene transition. The spatial pattern of peak hydroclimate anomalies matches the conditions seen in years with a weak Mozambique Channel Trough (MCT), suggesting the hydroclimate event may have been a time with more frequent weak MCT occurrences. Weak MCT years are associated with a northerly position of the summer west Indian Ocean ITCZ. However, many regional hydroclimate anomalies fail to provide evidence of an abrupt 4.2 ka event. Hydroclimate changes at the Mid- to Late-Holocene transition are typically gradual and consistently begin earlier than the abrupt 4.2 ka event, casting doubt as to whether the 4.2 ka event could be the cause of regional hydroclimate anomalies at this time. Assuming 4.2 ka event causality of the regional hydroclimate anomaly pattern would be an overinterpretation of existing data.

To improve our understanding of abrupt climate change under near modern boundary conditions, there is a need to pursue greater understanding of the mechanistic processes behind the 4.2 ka event. Given the difficulty of modelling an event that may not even have a direct forcing mechanism, this may be best achieved through investigating spatial patterns of climate anomalies in paleoclimate records. Enhanced regional syntheses that incorporate age uncertainty are required (Scroxton et al., 2022). Such syntheses are dependent on continued production of high-resolution, precisely dated, records capable of distinguishing the abrupt 4.26 to 3.97 kyr BP climate anomaly of the 4.2 ka event from other temporally proximate climatic changes such as at 4.0 kyr BP.

Author contributions

NS ran stable isotope and U–Th chemistry analysis of stalagmite AK1 in the labs of SJB and DM. NS conducted data analysis and was primarily responsible for writing the manuscript. SJB and DM conducted preliminary laboratory analysis and helped write the manuscript. LRG contributed to the manuscript at all stages. SJB, LRG, LR and PF conducted the fieldwork and speleothem collection. BT and PF ran additional U–Th chemistry analysis of stalagmite AK1. All authors contributed to editing the manuscript.

Declaration of competing interest

The authors declare that they have no known competing financial interests or personal relationships that could have appeared to influence the work reported in this paper.

Data availability

New data from stalagmite AK1 are available at the NOAA Paleoclimatology Database: https://www.ncdc.noaa.gov/paleo/study/37062 and have been submitted to the SISAL database for future release. Previously published data used in this study can be found in the following repositories. The **SISAL Database:** Rodrigues LAVI-4: entity ID 469; Cold Air Cave T5: entity ID 45; Cold Air Cave T8: entity ID 48; Sanbao SB-26: entity ID 296; Dongge D4: entity ID 446; Sahiya SAH-2: entity ID 478, Sahiya SAH-3: entity ID 479; Huagapo P09-H2: entity ID: 509. The **NOAA Paleoclimatology Database:** Kilimanjaro: study 2466; Lake Challa: studies 13539 and 10889; Burundi composite pollen-based precipitation estimate: study 6213; Lake Masoko: study 6072; Lake Malawi: study 5456. **Pangaea:** Mkhuze Delta MKD-1: study 922249 and 922247. **Mendeley Data:** Lake Muzi MZ4: Humphries et al. (2019) http://doi.org/10.17632/sjz3xhkkk8.1. **Not in public repositories:** records from Anjohibe (ANJ94-5) and Tatos Basin.

Acknowledgements

NS, SJB and DM acknowledge support from NSF award AGS-1702891/1702691, LRG and SJB from NSF award BCS-1750598 and DM from NSF award EAR-1439559 and the MIT Ferry Fund. Fieldwork in Madagascar was conducted under a collaborative accord for paleobiological and paleoclimatological research between the University of Antananarivo (Mention Bassins sédimentaires, Evolution, Conservation) and the University of Massachusetts Amherst (Department of Anthropology and Department of Geosciences). We thank the Ministry of Higher Education and Scientific Research, the Ministry of Mines and Strategic Resources, and the Ministry of Culture and Communication for permits to let us conduct field research in Madagascar.

References

Alley, R.B., Mayewski, P.A., Sowers, T., Stuiver, M., Taylor, K.C., Clark, P.U., 1997. Holocene climatic instability: a prominent, widespread event 8200 yr ago. Geology 25 (6), 483–486. https://doi.org/10.1130/0091-7613(1997)025<0483:HCIAPW>2.3.CO, 2.

Alley, R.B., Ágústsdóttir, A.M., 2005. The 8k event: cause and consequences of a major Holocene abrupt climate change. Quat. Sci. Rev. 24 (10–11), 1123–1149. https://doi.org/10.1016/j.quascirev.2004.12.004.

Baker, A., Genty, D., Dreybrodt, W., Barnes, W.L., 1998. Testing theoretically predicted stalagmite growth rate with recent annually laminated samples: implications for past stalagmite deposition. Geochem. Cosmochim. Acta 62 (3), 393–404. https://doi.org/10.1016/S0016-7037(97)00343-8.

Barber, D.C., Dyke, A., Hillaire-Marcel, C., Jennings, A.E., Andrews, J.T., Kerwin, M.W., Bilodeau, G., McNeely, R., Southon, J., Morehead, M.D., 1999. Forcing of the cold event of 8,200 years ago by catastrophic drainage of Laurentide lakes. Nature 400 (6742), 344–348. https://doi.org/10.1038/22504.

Barimalala, R., Desbiolles, F., Blamey, R.C., Reason, C., 2018. Madagascar influence on the South Indian Ocean convergence zone, the Mozambique Channel Trough and southern African rainfall, 380–11,389 Geophys. Res. Lett. 45 (20), 11. https://doi.org/10.1029/2018GL079964.

Barimalala, R., Blamey, R.C., Desbiolles, F., Reason, C.J.C., 2020. Variability in the Mozambique Channel Trough and impacts on Southeast African rainfall. J. Clim. 33 (2), 749–765. https://doi.org/10.1175/jcli-d-19-0267.1.

Bini, M., Zanchetta, G., Perşoiu, A., Cartier, R., Catala, A., Cacho, I., Dean, J.R., Di Rita, F., Drysdale, R.N., Finné, M., Isola, I., Jalali, B., Lirer, F., Magri, D., Masi, A., Marks, L., Mercuri, A.M., Peyron, O., Sadori, L., Sicre, M.-A., Welc, F., Zielhofer, C., Brisset, E., 2019. The 4.2 ka BP Event in the Mediterranean region: an overview. Clim. Past 15 (2), 555–577. https://doi.org/10.5194/cp-15-555-2019.

Bond, G., 1997. A pervasive millennial-scale cycle in North Atlantic Holocene and glacial climates. Science 278 (5341), 1257–1266. https://doi.org/10.1126/science.278.5341.1257.

Bond, G., Kromer, B., Beer, J., Muscheler, R., Evans, M.N., Showers, W., Hoffmann, S., Lotti-Bond, R., Hajdas, I., Bonani, G., 2001. Persistent solar influence on North Atlantic climate during the Holocene. Science 294 (5549), 2130–2136. https://doi.org/10.1126/science.1065680.

Bonnefille, R., Chalie, F., 2000. Pollen-inferred precipitation time-series from equatorial mountains, Africa, the last 40 kyr BP. Global Planet. Change 26 (1–3), 25–50. https://doi.org/10.1016/S0921-8181(00)00032-1.

Bradley, R.S., Bakke, J., 2019. Is there evidence for a 4.2 ka BP event in the northern North Atlantic region? Clim. Past 151665–151676. https://doi.org/10.5194/cp-15-1665-2019.

Broccoli, A.J., Dahl, K.A., Stouffer, R.J., 2006. Response of the ITCZ to northern hemisphere cooling. Geophys. Res. Lett. 33 (1), L01702. https://doi.org/10.1029/2005GL024546.

Bronk Ramsey, C., 2008. Deposition models for chronological records. Quat. Sci. Rev. 27 (1–2), 42–60. https://doi.org/10.1016/j.quascirev.2007.01.019.

Brouard, E., Roy, M., Godbout, P.M., Veillette, J.J., 2021. A framework for the timing of the final meltwater outbursts from glacial Lake Agassiz-Ojibway. Quat. Sci. Rev. 272, 107629. https://doi.org/10.1016/j.quascirev.2021.107269.

Carolin, S.A., Walker, R.T., Day, C.C., Ersek, V., Sloan, R.A., Dee, M.W., Talebian, M., Henderson, G.M., 2019. Precise timing of abrupt increase in dust activity in the Middle East coincident with 4.2 ka social change. Proc. Natl. Acad. Sci. U.S.A. 116 (1), 67–72. https://doi.org/10.1073/pnas.1808103115.

Castañeda, I.S., Werne, J.P., Johnson, T.C., 2007. Wet and arid phases in the southeast African tropics since the last glacial maximum. Geology 35 (9), 823–826. https://doi.org/10.1130/G23916A.1.

Cheng, H., Lawrence Edwards, R., Edwards, R.L., Shen, C.-C., Polyak, V.J., Asmerom, Y., Woodhead, J., Hellstrom, J., Wang, Y., Kong, X., Spötl, C., Wang, X.,

Alexander, Calvin, Jr, E., 2013. Improvements in 230Th dating, 230Th and 234U half-life values, and U–Th isotopic measurements by multi-collector inductively coupled plasma mass spectrometry. Earth Planet Sci. Lett. 371, 82–91. https://doi.org/10.1016/j.epsl.2013.04.006, 372.

Cook, B.I., Mankin, J.S., Anchukaitis, K.J., 2018. Climate change and drought: from past to future. Curr. Clim. Change Rep. 4, 164–179. https://doi.org/10.1007/s40641-018-0093-2.

de Boer, E.J., Tjallingii, R., Vélez, M.I., Rijsdijk, K.F., Vlug, A., Reichart, G.-J., Prendergast, A.L., de Louw, P.G.B., Florens, F.B.V., Baider, C., Hooghiemstra, H., 2014. Climate variability in the SW Indian Ocean from an 8000-yr long multi-proxy record in the Mauritian lowlands shows a middle to late Holocene shift from negative IOD-state to ENSO-state. Quat. Sci. Rev. 86, 175–189. https://doi.org/10.1016/j.quascirev.2013.12.026.

Dee, D.P., Uppala, S.M., Simmons, A.J., Berrisford, P., Poli, P., Kobayashi, S., Andrae, U., Balmaseda, M.A., Balsamo, G., Bauer, P., Bechtold, P., Beljaars, A.C.M., van de Berg, L., Bidlot, J., Bormann, N., Delsol, C., Dragani, R., Fuentes, M., Geer, A.J., Haimberger, L., Healy, S.B., Hersbach, H., Hólm, E.V., Isaksen, L., Kållberg, P., Köhler, M., Matricardi, M., McNally, A.P., Monge-Sanz, B.M., Morcrette, J.-J., Park, B.-K., Peubey, C., de Rosnay, P., Tavolato, C., Thépaut, J.-N., Vitart, F., 2011. The ERA-Interim reanalysis: configuration and performance of the data assimilation system. Q. J. R. Meteorol. Soc. 137 (656), 553–597. https://doi.org/10.1002/qj.828.

Denniston, R.F., Wyrwoll, K.-H., Polyak, V.J., Brown, J.R., Asmerom, Y., Wanamaker Jr., A.D., LaPointe, Z., Ellerbroek, R., Barthelmes, M., Cleary, D., Cugley, J., Woods, D., Humphreys, W.F., 2013. A Stalagmite record of Holocene Indonesian–Australian summer monsoon variability from the Australian tropics. Quat. Sci. Rev. 78, 155–168. https://doi.org/10.1016/j.quascirev.2013.08.004.

Dong, J., Wang, Y., Cheng, H., Hardt, B., Edwards, R.L., Kong, X., Wu, J., Chen, S., Liu, D., Jiang, X., Zhao, K., 2010. A high-resolution stalagmite record of the Holocene East Asian monsoon from Mt Shennongjia, central China. Holocene 20 (2), 257–264. https://doi.org/10.1177/0959683609350393.

Dorale, J.A., Liu, Z., 2009. Limitations of hendy test criteria in judging the paleoclimatic suitability of speleothems and the need for replication. J. Cave Karst Stud. 71 (1), 73–80.

Dreybrodt, W., 1999. Chemical kinetics, speleothem growth and climate. Boreas 28 (3), 347–356. https://doi.org/10.1111/j.1502-3885.1999.tb00224.x.

Duan, P., Li, H., Sinha, A., Voarintsoa, N.R.G., Kathayat, G., Hu, P., Zhang, H., Ning, Y., Cheng, H., 2021. The timing and structure of the 8.2 ka event revealed through high-resolution speleothem records from northwestern Madagascar. Quat. Sci. Rev. 268, 107104, 1. 1016/j.quascirev.2021.107104.

Dykoski, C., Edwards, R., Cheng, H., Yuan, D., Cai, Y., Zhang, M., Lin, Y., Qing, J., An, Z., Revenaugh, J., 2005. A high-resolution, absolute-dated Holocene and deglacial Asian monsoon record from Dongge Cave, China. Earth Planet Sci. Lett. 233 (2), 71–86. https://doi.org/10.1016/j.epsl.2005.01.036.

Fairchild, I.J., Baker, A., 2012. Speleothem Science: from Process to Past Environments. Blackwell Publishing Ltd.

Fitchett, J.M., Mackay, A.W., Grab, S.W., Bamford, M.K., 2017. Holocene climatic variability indicated by a multi-proxy record from southern Africa's highest wetland. Holocene 27 (5), 638–650. https://doi.org/10.1177/0959683616670467.

Fleitmann, D., Burns, S.J., Mudelsee, M., Neff, U., Kramers, J., Mangini, A., Matter, A., 2003. Holocene forcing of the Indian Monsoon recorded in a stalagmite from Southern Oman. Science 300 (5626), 1737–1739. https://doi.org/10.1126/science.1083130.

Gagan, M.K., Hendy, E.J., Haberle, S.G., Hantoro, W.S., 2004. Post-glacial evolution of the indo-pacific warm pool and El niño-southern oscillation. Quat. Int. 118–119, 127–143. https://doi.org/10.1016/s1040-6182(03)00134-4.

Garcin, Y., Williamson, D., Taieb, M., Vincens, A., Mathé, P.-E., Majule, A., 2006. Centennial to millennial changes in maar-lake deposition during the last 45,000 years in tropical Southern Africa (Lake Masoko, Tanzania). Palaeogeogr. Palaeoclimatol. Palaeoecol. 239 (3–4), 334–354. https://doi.org/10.1016/j.palaeo.2006.02.002.

Gibert, E., Bergonzini, L., Massault, M., Williamson, D., 2002. AMS-14C chronology of 40.0 cal ka BP continuous deposits from a crater lake (Lake Massoko, Tanzania): modern water balance and environmental implications. Palaeogeogr. Palaeoclimatol. Palaeoecol. 187 (3–4), 307–322. https://doi.org/10.1016/S0031-0182(02)00483-2.

Giosan, L., Orsi, W.D., Coolen, M., Wuchter, C., Dunlea, A.G., Thirumalai, K., Munoz, S.E., Clift, P.D., Donnelly, J.P., Galy, V., Fuller, D.Q., 2018. Neoglacial climate anomalies and the Harappan metamorphosis. Clim. Past 14 (11), 1669–1686. https://doi.org/10.5194/cp-14-1669-2018.

Gupta, A.K., Anderson, D.M., Overpeck, J.T., 2003. Abrupt changes in the asian southwest monsoon during the Holocene and their links to the North Atlantic ocean. Nature 421 (6921), 354–357. https://doi.org/10.1038/nature01340.

Hanasaki, N., Fujimori, S., Yamamoto, T., Yoshikawa, S., Masaki, Y., Kainuma, M., Kanamori, Y., Masui, T., Takahashi, T., Kanae, S., 2013. A global water scarcity assessment under Shared Socio-economic Pathways–Part 2: water availability and scarcity. Hydrol. Earth Syst. Sci. 17, 2393–2413. https://doi.org/10.5194/hess-17-2393-2013.

Helama, S., Oinonen, M., 2019. Exact dating of the Meghalayan lower boundary based on high-latitude tree-ring isotope chronology. Quat. Sci. Rev. 214, 178–184. https://doi.org/10.1016/j.quascirev.2019.04.013.

Hersbach, H., Bell, B., Berrisford, P., Biavati, G., Horányi, A., Muñoz Sabater, J., Nicolas, J., Peubey, C., Radu, R., Rozum, I., Schepers, D., Simmons, A., Soci, C., Dee, D., Thépaut, J.-N., 2019a. ERA5 monthly averaged data on single levels from 1979 to present. Copernicus Clim Change Ser (C3S) Climate Data Store (CDS). https://doi.org/10.24381/cds.f17050d7.

Hersbach, H., Bell, B., Berrisford, P., Biavati, G., Horányi, A., Muñoz Sabater, J., Nicolas, J., Peubey, C., Radu, R., Rozum, I., 2019b. ERA5 Monthly Averaged Data on Pressure Levels from 1979 to Present, Copernicus Climate Change Service (C3S) Climate Data Store (CDS). https://doi.org/10.24381/cds.6860a573.

Hersbach, H., Bell, B., Berrisford, P., Hirahara, S., Horányi, A., Muñoz-Sabater, J., Nicolas, J., Peubey, C., Radu, R., Schepers, D., 2020. The ERA5 global reanalysis. Q. J. R. Meteorol. Soc. 146 (730), 1999–2049.

Höflmayer, F., 2017. The late third millennium B.C. In the ancient near east and eastern mediterranean. In: Höflmayer, F. (Ed.), A Time of Collapse and Transformation. Oriental Institute Seminars, pp. 1–30.

Holmgren, K., Lee-Thorp, J.A., Cooper, G.R.J., Lundblad, K., Partridge, T.C., Scott, L., Sithaldeen, R., Talma, A.S., Tyson, P.D., 2003. Persistent millennial-scale climatic variability over the past 25,000 years in Southern Africa. Quat. Sci. Rev. 22 (21–22), 2311–2326. https://doi.org/10.1016/S0277-3791(03)00204-X.

Humphries, M., Green, A., Higgs, C., Strachan, K., Hahn, A., Pillay, L., Zabel, M., 2020. High-resolution geochemical records of extreme drought in southeastern Africa during the past 7000 years. Quat. Sci. Rev., 236106294 https://doi.org/10.1016/j.quascirev.2020.106294.

Humphries, M.S., Kirsten, K.L., McCarthy, T.S., 2019. Rapid changes in the hydroclimate of southeast Africa during the mid-to late-Holocene. Quat. Sci. Rev. 212, 178–186. https://doi.org/10.1016/j.quascirev.2019.04.006.

Jaffey, A.H., Flynn, K.F., Glendenin, L.E., Bentley, W.C., Essling, A.M., 1971. Precision measurement of half-Lives and specific activities of ^{235}U and ^{238}U. Phys. Rev. C 4 (5), 1889–1906. https://doi.org/10.1103/PhysRevC.4.1889.

Johnson, T.C., Brown, E.T., McManus, J., Barry, S., Barker, P., Gasse, F., 2002. A high-resolution paleoclimate record spanning the past 25,000 years in southern East Africa. Science 296 (5565), 113–132. https://doi.org/10.1126/science.1070057.

Jury, M.R., Pathack, B., 1991. A study of climate and weather variability over the tropical southwest Indian Ocean. Meteorol. Atmos. Phys. 47 (1), 37–48. https://doi.org/10.1007/BF01025825.

Jury, M.R., Parker, B.A., Raholijao, N., Nassor, A., 1995. Variability of summer rainfall over Madagascar: climatic determinants at interannual scales. Int. J. Climatol. 15 (12), 1323–1332. https://doi.org/10.1002/joc.3370151203.

Kaniewski, D., Marriner, N., Cheddadi, R., Guiot, J., Campo, E.V., 2018. The 4.2 ka BP event in the Levant. Clim. Past 14 (10), 1529–1542. https://doi.org/10.5194/cp-14-1529-2018.

Kanner, L.C., Burns, S.J., Cheng, H., Edwards, R.L., Vuille, M., 2013. High-resolution variability of the South American summer monsoon over the last seven millennia: insights from a speleothem record from the central Peruvian Andes. Quat. Sci. Rev. 75, 1–10. https://doi.org/10.1016/j.quascirev.2013.05.008.

Kathayat, G., Cheng, H., Sinha, A., Yi, L., Li, X., Zhang, H., Li, H., Ning, Y., Edwards, R.L., 2017. The Indian monsoon variability and civilization changes in the Indian subcontinent. Sci. Adv. 3 (12), e1701296. https://doi.org/10.1126/sciadv.1701296.

Kim, S.-T., O'Neil, J.R., Hillaire-Marcel, C., Mucci, A., 2007. Oxygen isotope fractionation between synthetic aragonite and water: influence of temperature and Mg2+ concentration. Geochem. Cosmochim. Acta 71 (19), 4704–4715. https://doi.org/10.1016/j.gca.2007.04.019.

Konapala, G., Mishra, A.K., Wada, Y., Mann, M.E., 2020. Climate change will affect global water availability through compounding changes in seasonal precipitation and evaporation. Nat. Commun. 113044. https://doi.org/10.1038/s41467-020-16757-w.

Koseki, S., Bhatt, B.C., 2018. Unique relationship between tropical rainfall and SST to the north of the Mozambique Channel in boreal winter. Int. J. Climatol. 38, e378–e387. https://doi.org/10.1002/joc.5378.

Lachniet, M.S., 2009. Climatic and environmental controls on speleothem oxygen-isotope values. Quat. Sci. Rev. 28 (5–6), 412–432. https://doi.org/10.1016/j.quascirev.2008.10.021.

Laumanns, M., Gebauer, H., 1993. Namoroka 1992. Expedition to the karst of Namoroka and Narinda, Madagascar. International Caver 6, 30–36.

Li, H., Cheng, H., Sinha, A., Kathayat, G., Spötl, C., André, A.A., Meunier, A., Biswas, J., Duan, P., Ning, Y., Edwards, R.L., 2018. Hydro-climatic variability in the southwestern Indian Ocean between 6000 and 3000 years ago. Clim. Past 14 (12), 1881–1891. https://doi.org/10.5194/cp-14-1881-2018.

Liu, X., Rendle-Bühring, R., Kuhlmann, H., Kuhlmann, H., Li, A., 2017. Two phases of the Holocene east african humid period: inferred from a high-resolution geochemical record off Tanzania. Earth Planet Sci. Lett. 460, 123–134. https://doi.org/10.1016/j.epsl.2016.12.016.

Loucks, D.P., 2022. Meeting climate change challenges: searching for more adaptive and innovative decisions. Water Resour. Manag. https://doi.org/10.1007/s11269-022-03227-9.

MacDonald, G., 2011. Potential influence of the Pacific Ocean on the Indian summer monsoon and Harappan decline. Quat. Int. 229 (1–2), 140–148. https://doi.org/10.1016/j.quaint.2009.11.012.

Macron, Clémence, Pohl, Benjamin, Richard, Yves, Bessafi, Miloud, 2014. How do tropical temperate troughs form and develop over Southern Africa? J. Clim. 27 (4), 1633–1647. https://doi.org/10.1175/jcli-d-13-00175.1.

Macron, C., Richard, Y., Garot, T., Bessafi, M., Pohl, B., Ratiarison, A., Razafindrabe, A., 2016. Intraseasonal rainfall variability over Madagascar. Mon. Weather Rev. 144 (5), 1877–1885. https://doi.org/10.1175/mwr-d-15-0077.1.

Marchant, R., Hooghiemstra, H., 2004. Rapid environmental change in African and South American tropics around 4000 years before present: a review. Earth Sci. Rev. 66 (3–4), 217–260. https://doi.org/10.1016/j.earscirev.2004.01.003.

Markowska, M., Cuthbert, M.O., Baker, A., Treble, P.C., Andersen, M.S., Adler, L., Griffiths, A., Frisia, S., 2020. Modern speleothem oxygen isotope hydroclimate records in water-limited SE Australia. Geochem. Cosmochim. Acta 270, 431–448. https://doi.org/10.1016/j.gca.2019.12.007.

Mayewski, P.A., Rohling, E.E., Stager, J.C., Karlén, W., Maasch, K.A., Meeker, L.D., Meyerson, E.A., Gasse, F., van Kreveld, S., Holmgren, K., Lee-Thorp, J., Rosqvist, G., Rack, F., Staubwasser, M., Schneider, R.R., Steig, E.J., 2004. Holocene climate variability. Quat. Res. 62 (3), 243–255. https://doi.org/10.1016/j.yqres.2004.07.001.

McDermott, F., 2004. Palaeo-climate reconstruction from stable isotope variations in speleothems: a review. Quat. Sci. Rev. 23 (7–8), 901–918. https://doi.org/10.1016/j.quascirev.2003.06.021.

McGee, D., Donohoe, A., Marshall, J., Ferreira, D., 2014. Changes in ITCZ location and cross-equatorial heat transport at the last glacial maximum, heinrich stadial 1, and the mid-holocene. Earth Planet Sci. Lett. 390, 69–79. https://doi.org/10.1016/j.epsl.2013.12.043.

Mickler, P.J., Stern, L.A., Banner, J.L., 2006. Large kinetic isotope effects in modern speleothems. Geol. Soc. Am. Bull. 118 (1–2), 65–81. https://doi.org/10.1130/B25698.1.

Middleton, G.D., 2018. Bang or whimper? Science 361 (6408), 1204–1205. https://doi.org/10.1126/science.aau8834.

Morrill, C., Anderson, D.M., Bauer, B.A., Buckner, R., Gille, E.P., Gross, W.S., Hartman, M., Shah, A., 2013. Proxy benchmarks for intercomparison of 8.2 ka simulations. Clim. Past 9 (1), 423–432.

Narisma, G.T., Foley, J.A., Licker, R., Ramankutty, N., 2007. Abrupt changes in rainfall during the twentieth century. Geophys. Res. Lett. 34, L06710. https://doi.org/10.1029/2006GL028628.

Nash, D.J., De Cort, G., Chase, B.M., Verschuren, D., Nicholson, S.E., Shanahan, T.M., Asrat, A., Lézine, A.-M., Grab, S.W., 2016. African hydroclimatic variability during the last 2000 years. Quat. Sci. Rev. 154, 1–22. https://doi.org/10.1016/j.quascirev.2016.10.012.

Ön, Z.B., Greaves, A.M., Akçer-Ön, S., Özeren, M.S., 2021. A Bayesian test for the 4.2 ka BP abrupt climatic change event in southeast Europe and southwest Asia using structural time series analysis of paleoclimate. Clim. Change 165, 7. https://doi.org/10.1007/s10584-021-03010-6.

Parker, S.E., Harrison, S.P., 2022. The timing, duration and magnitude of the 8.2 ka event in global speleothem records. Sci. Rep. 12, 10542. https://doi.org/10.1038/s41598-022-14684-y.

Railsback, L.B., Akers, P.D., Wang, L., 2013. Layer-bounding surfaces in stalagmites as keys to better paleoclimatological histories and chronologies. Int. J. Speleol. https://doi.org/10.5038/1827-806X.42.3.1.

Railsback, L.B., Liang, F., Brook, G.A., Voarintsoa, N.R.G., Sletten, H.R., Marais, E., Hardt, B., Cheng, H., Edwards, R.L., 2018. The timing, two-pulsed nature, and variable climatic expression of the 4.2 ka event: a review and new high-resolution stalagmite data from Namibia. Quat. Sci. Rev. 186, 78–90. https://doi.org/10.1016/j.quascirev.2018.02.015.

Railsback, L.B., Liang, F., Brook, G.A., Cheng, H., Edwards, R.L., 2022. Additional multi-proxy stalagmite evidence from northeast Namibia supports recent models of wetter conditions during the 4.2 ka Event in the Southern Hemisphere. Palaeogeogr. Palaeoclimatol. Palaeoecol., 586110756 https://doi.org/10.1016/j.palaeo.2021.110756.

Repinski, P., Holmgren, K., Lauritzen, S.E., Lee Thorp, J.A., 1999. A late Holocene climate record from a stalagmite, cold Air cave, northern province, South Africa. Palaeogeogr. Palaeoclimatol. Palaeoecol. 150 (4), 269–277. https://doi.org/10.1016/S0031-0182(98)00223-5.

Schott, F.A., McCreary Jr, J.P., 2001. The monsoon circulation of the Indian Ocean. Prog. Oceanogr. 51 (1), 1–123, 1. 1016/S0079-6611(01)00083-0.

Scroxton, N, Burns, S.J., McGee, D., Godfrey, L.R., Ranivoharimanana, L., Faina, P., Tiger, B.H., 2022. Tropical Indian Ocean basin hydroclimate at the Mid- to Late-Holocene transition and the Double Drying hypothesis. Quaternary Science Reviews. https://doi.org/10.1016/j.quascirev.2022.107837. In press.

Scroxton, N., Burns, S.J., McGee, D., Hardt, B., Godfrey, L.R., Ranivoharimanana, L., Faina, P., 2017. Hemispherically in-phase precipitation variability over the last 1700 years in a Madagascar speleothem record. Quat. Sci. Rev. 164, 25–36. https://doi.org/10.1016/j.quascirev.2017.03.017.

Scroxton, N., Burns, S.J., McGee, D., Hardt, B., Godfrey, L.R., Ranivoharimanana, L., Faina, P., 2019. Competing temperature and atmospheric circulation effects on southwest Madagascan rainfall during the Last Deglaciation. Paleoceanogr. Paleoclimatol. 34 (2), 275–286. https://doi.org/10.1029/2018pa003466.

Staubwasser, M., Weiss, H., 2006. Holocene climate and cultural evolution in late prehistoric–early historic west asia. Quat. Res. 66 (3), 372–387. https://doi.org/10.1016/j.yqres.2006.09.001.

Tarutani, T., Clayton, R.N., Mayeda, T.K., 1969. The effect of polymorphism and magnesium substitution on oxygen isotope fractionation between calcium carbonate and water. Geochem. Cosmochim. Acta 33 (8), 987–996. https://doi.org/10.1016/0016-7037(69)90108-2.

Thomas, D.S.G., Bailey, R., Shaw, P.A., Durcan, J.A., Singarayer, J.S., 2009. Late Quaternary highstands at Lake Chilwa, Malawi: frequency, timing and possible forcing mechanisms in the last 44ka. Quat. Sci. Rev. 28 (5), 526–539. https://doi.org/10.1016/j.quascirev.2008.10.023.

Thompson, L.G., Mosley-Thompson, E., Davis, M.E., Henderson, K.A., Brecher, H.H., Zagorodnov, V.S., Mashiotta, T.A., Lin, P.N., Mikhalenko, V.N., Hardy, D.R., Beer, J., 2002. Kilimanjaro ice core records: evidence of Holocene climate change in tropical Africa. Science 298 (5593), 589–593. https://doi.org/10.1126/science.1073198.

Tierney, J.E., Russell, J.M., Sinninghe Damsté, J.S., Huang, Y., Verschuren, D., 2011. Late quaternary behavior of the east african monsoon and the importance of the Congo Air boundary. Quat. Sci. Rev. 30 (7–8), 798–807. https://doi.org/10.1016/j.quascirev.2011.01.017.

Toth, L.T., Aronson, R.B., Vollmer, S.V., Hobbs, J.W., Urrego, D.H., Cheng, H., Enochs, I.C., Combosch, D.J., Van Woesik, R., Macintyre, I.G., 2012. ENSO drove 2500-year collapse of eastern Pacific coral reefs. Science 337 (6090), 81–84. https://doi.org/10.1126/science.1221168.

Toth, L.T., Aronson, R.B., 2019. The 4.2 ka event, ENSO, and coral reef development. Clim. Past 15 (1), 105–119. https://doi.org/10.5194/cp-15-105-2019.

Verschuren, D., Damsté, J.S.S., Moernaut, J., Kristen, I., Blaauw, M., Fagot, M., Haug, G.H., van Geel, B., De Batist, M., Barker, P., Vuille, M., Conley, D.J., Olago, D.O., Milne, I., Plessen, B., Eggermont, H., Wolff, C., Hurrell, E., Ossebaar, J., Lyaruu, A., van der Plicht, J., Cumming, B.F., Brauer, A., Rucina, S.M., Russell, J.M., Keppens, E., Hus, J., Bradley, R.S., Leng, M., Mingram, J., Nowaczyk, N.R., 2009. Half-precessional dynamics of monsoon rainfall near the East African Equator. Nature 462 (7273), 637–641. https://doi.org/10.1038/nature08520.

Voarintsoa, N.R.G., Wang, L., Railsback, L.B., Brook, G.A., Liang, F., Cheng, H., Edwards, R.L., 2017. Multiple proxy analyses of a U/Th-dated stalagmite to reconstruct paleoenvironmental changes in northwestern Madagascar between 370CE and 1300CE. Palaeogeogr. Palaeoclimatol. Palaeoecol. 469, 138–155. https://doi.org/10.1016/j.palaeo.2017.01.003.

Voarintsoa, N.R.G., Matero, I.S.O., Railsback, L.B., Gregoire, L.J., Tindall, J., Sime, L., Cheng, H., Edwards, R.L., Brook, G.A., Kathayat, G., Li, X., Michel Rakotondrazafy, A.F., Madison Razanatseheno, M.O., 2019. Investigating the 8.2 ka event in northwestern Madagascar: insight from data–model comparisons. Quat. Sci. Rev. 204, 172–186. https://doi.org/10.1016/j.quascirev.2018.11.030.

Voarintsoa, N.R.G., Ratovonanahary, A.L.J., Rakotovao, A.Z.M., Bouillon, S., 2021. Understanding the linkage between regional climatology and cave geochemical parameters to calibrate speleothem proxies in Madagascar. Sci. Total Environ. 784, 147181.

Voosen, P., 2018. New geological age comes under fire. Science 361 (6402), 537–538. https://doi.org/10.1126/science.361.6402.537.

Walker, M., Head, M.H., Berklehammer, M., Bjorck, S., Cheng, H., Cwynar, L., Fisher, D., Gkinis, V., Long, A., Lowe, J., Newnham, R., Rasmussen, S.O., Weiss, H., 2018. Formal ratification of the subdivision of the Holocene series/epoch (quaternary system/period): two new global boundary stratotype sections and points (GSSPs) and three new stages/subseries. Episodes 41 (4), 213–223. https://doi.org/10.18814/epiiugs/2018/018016.

Wang, B., Ding, Q., 2008. Global monsoon: dominant mode of annual variation in the tropics. Dyn. Atmos Oceans 44 (3–4), 165–183. https://doi.org/10.1016/j.dynatmoce.2007.05.002.

Wang, L., Brook, G.A., Burney, D.A., Voarintsoa, N.R.G., Liang, F., Cheng, H., Edwards, R.L., 2019. The African Humid Period, rapid climate change events, the timing of human colonization, and megafaunal extinctions in Madagascar during the Holocene: evidence from a 2m Anjohibe Cave stalagmite. Quat. Sci. Rev. 210, 136–153. https://doi.org/10.1016/j.quascirev.2019.02.004.

Wang, S., Ge, Q., Wang, F., Wen, X., Huang, J., 2013. Abrupt climate changes of Holocene. Chin. Geogr. Sci. 23 (1), 1–12. https://doi.org/10.1007/s11769-013-0591-z.

Wanner, H., Solomina, O., Grosjean, M., Ritz, S.P., Jetel, M., 2011. Structure and origin of Holocene cold events. Quat. Sci. Rev. 30 (21–22), 3109–3123. https://doi.org/10.1016/j.quascirev.2011.07.010.

Weiss, H., Courty, M.-A., Wetterstrom, W., Guichard, F., Senior, L., Meadow, R., Curnow, A., 1993. The genesis and collapse of third millennium north Mesopotamian civilization. Science 261 (5124), 995–1004. https://doi.org/10.1126/science.261.5124.995.

Weiss, H., 1997. Late Third Millennium Abrupt Climate Change and Social Collapse in West Asia and Egypt. Springer Berlin, Heidelberg, pp. 711–723.

Weldeab, S., Lea, D.W., Oberhänsli, H., Schneider, R.R., 2014. Links between southwestern tropical Indian Ocean SST and precipitation over southeastern Africa over the last 17kyr. Palaeogeogr. Palaeoclimatol. Palaeoecol. 410, 200–212. https://doi.org/10.1016/j.palaeo.2014.06.001.

Xie, P., Arkin, P.A., 1997. Global precipitation: a 17-year monthly analysis based on gauge observations, satellite estimates, and numerical model outputs. Bull. Am. Meterol. 78 (11), 2539–2558. https://doi.org/10.1175/1520-0477(1997)078<2539:gpayma>2.0.co, 2.

Yan, M., Liu, J., 2019. Physical processes of cooling and mega-drought during the 4.2 ka BP event: results from TraCE-21ka simulations. Clim. Past 15 (1), 265–277. https://doi.org/10.5194/cp-15-265-2019.

Zanchetta, G., Isola, I., Drysdale, R.N., Bini, M., Baneschi, I., Hellstrom, J., 2016. The so-called "4.2 event" in the central mediterranean and its climatic teleconnections. Alp. Mediterr. Quat. 29, 5–17.

Zhang, R., Delworth, T.L., 2005. Simulated tropical response to a substantial weakening of the Atlantic thermohaline circulation. J. Clim. 18 (12), 1853–1860. https://doi.org/10.1175/jcli3460.1.

Zinke, J., Dullo, W.-C., Heiss, G.A., Eisenhauer, A., 2004. ENSO and Indian Ocean subtropical dipole variability is recorded in a coral record off southwest Madagascar for the period 1659 to 1995. Earth Planet Sci. Lett. 228 (1–2), 177–194. https://doi.org/10.1016/j.epsl.2004.09.028.